Introductory Solid-State Physics

Lecture notes

Alexander Tsirlin

Leipzig University

work in progress, use with caution
report any comments and errors to alexander.tsirlin@uni-leipzig.de

February 4, 2024

Contents

1. Bravais lattice, or how to pack a crystal? 4
- 1.1. Bravais lattice and unit cell
- 1.2. Close packing and structures of metals
- 1.3. Electron microscopy

2. Symmetry as the guiding principle 7
- 2.1. Symmetry operations
- 2.2. Translational symmetry: lattice centering
- 2.3. Rotational symmetry and birefringence
- 2.4. Reflection and inversion symmetry
- 2.5. Neumann's principle
- 2.6. Rotation vs. periodicity

3. Systematics of crystals: symmetry groups 11
- 3.1. Point symmetry operations
- 3.2. Point groups and crystal classes. Polarity
- 3.3. Crystal systems
- 3.4. Open symmetry elements
- 3.5. Chirality
- 3.6. Circular birefringence and dichroism
- 3.7. Space groups

4. Unpacking the crystal structure 17
- 4.1. Atomic coordinates and Wyckoff positions
- 4.2. Crystal structure
- 4.3. Bragg's law
- 4.4. Scattering experiments and x-ray diffraction
- 4.5. Lattice planes and Miller indices
- 4.6. Crystal faces and crystal directions

5. Spaces of crystallography: Reciprocal lattice 22
- 5.1. Laue condition
- 5.2. Reciprocal lattice
- 5.3. Relation to Bragg's law
- 5.4. Aperiodic crystals

6. Structure factor: All shades of diffraction 26
- 6.1. Structure factor
- 6.2. Atomic approximation
- 6.3. Extinction conditions
- 6.4. Crystal structure determination
- 6.5. Atomic form factors
- 6.6. Neutron diffraction

7. Bonding in crystals: ionic 31
- 7.1. Types of chemical bonding
- 7.2. Cohesive and lattice energies
- 7.3. Madelung constant
- 7.4. Born-Landé equation
- 7.5. Bulk modulus
- 7.6. Ionic radius and Pauling's rule
- 7.7. Ionic crystals as close-packed structures

8. Bonding in crystals: covalent, metallic, and van der Waals 36
8.1. Covalent crystals
8.2. Metallic crystals
8.3. Polymorphism
8.4. van der Waals radius and Lennard-Jones potential
8.5. Lattice energy
8.6. Bulk modulus

9. Mechanical properties 39
9.1. Hydrostatic pressure, Equation of state
9.2. Uniaxial pressure
9.3. Shear deformation
9.4. Stress and strain tensors
9.5. Elastic constants
9.6. Plastic deformation

10. Dielectric properties 44
10.1. Permittivity
10.2. Dielectric loss
10.3. Induced dipoles and polarizability
10.4. Local electric field
10.5. Clausius-Mossotti relation
10.6. Permanent dipoles, Debye relaxation
10.7. Cole-Cole plots

11. Phonons and sound 50
11.1. Underlying approximations
11.2. Monoatomic chain
11.3. Elastic waves and sound
11.4. Longitudinal and transverse phonons
11.5. Diatomic chain
11.6. Acoustic and optical phonons

12. Phonons and light 55
12.1. Refractive index and reflectivity
12.2. Fluctuating dipoles
12.3. LO vs. TO
12.4. Interaction with light, polaritons
12.5. Lyddane-Sachs-Teller relation
12.6. Infra-red active phonon modes

13. Phonons and the reciprocal lattice 61
13.1. Brillouin zone
13.2. Dynamical matrix

A. Electrodynamics 62
A.1. Maxwell's equations
A.2. Electromagnetic waves
A.3. Longitudinal waves

B. Thermodynamics 64

C. List of experimental techniques 64

Introduction

Condensed matter represents the largest sub-field of physics. It is not without a reason, because condensed matter, or colloquially *cond-mat*, covers many aspects of physics that we encounter in our daily life. While different branches of condensed-matter research have many concepts and experimental techniques in common, they are also highly diverse, especially when it comes to research objects.

One generally distinguishes research on *soft matter* (polymers, gels, membranes, cellular structures) from *hard condensed matter* or simply *solid-state physics* that addresses properties of solid materials. This distinction is in fact rather subtle. It goes back to the different dynamics of "soft" and "hard" systems. Soft matter shows pronounced dynamics at ambient conditions, it does not have a "fixed" structure, which is integral to solids. However, soft-matter objects may become crystalline and turn into solids, whereas solids may show certain features of a liquid.

Solid-state materials are variable too. They can be *crystalline* or *amorphous*. Crystalline solids feature long-range-ordered structures (crystal structures) that are typically periodic.[1] By contrast, amorphous solids lack long-range order in any form, although they still show some organization on the short-range scale.

Traditionally, solid-state physics has been developed for crystalline materials. Some of its findings can be extended to amorphous materials too, but many of the key concepts, such as band structure, are properly defined for crystalline materials only. In fact, they strongly rely on periodicity and would require some re-thinking even for aperiodic crystals.

The **content** of these lecture notes splits into three parts:

- **Structure of crystals** (Chapters 1 to 6). Here, we discuss how crystals are organized and use *symmetry* for classification of crystals and their properties.
- **Atoms in crystals** (Chapters...). This part concentrates on *lattice degrees of freedom*, namely, bonding between the atoms as well as atomic vibrations and motions, and how all of this contributes to different crystal properties.
- **Electrons in crystals** (Chapters...) This part will mostly address metals and analyze how *electronic degrees of freedom* (free or, more precisely, itinerant electrons) affect different physical properties.

Many of the crystals also have *spin degrees of freedom*, but we disregard those for the sake of simplicity. Magnetic properties of solids are addressed in a separate module.

Hyperlinks are highlighted in blue color. They will usually direct you to useful web resources or an additional information on the topic.

[1] A few examples of aperiodic crystalline solids will be introduced in Chapters 2 and 5.

1. Bravais lattice, or how to pack a crystal?

1.1. Bravais lattice and unit cell

Periodic pattern of the crystal can be described by a *Bravais lattice* defined as a set of points

$$\mathbf{R} = n_1\mathbf{a} + n_2\mathbf{b} + n_3\mathbf{c} \tag{1.1}$$

where n_1, n_2, n_3 are integers and $\mathbf{a}$, $\mathbf{b}$, $\mathbf{c}$ are three vectors that do not lie in the same plane. They are known as *lattice translations* or *lattice vectors*. The parallelepiped spun by these three vectors is the repetition unit of the lattice or its *unit cell* with the *lattice parameters* (a, b, c) and *lattice angles* (α, β, γ). It is customary to define the angle between $\mathbf{b}$ and $\mathbf{c}$ as α, the angle between $\mathbf{a}$ and $\mathbf{c}$ as β, and the angle between a and b as γ.

Not every lattice is a Bravais lattice. Consider for example hexagonal (honeycomb) lattice, one of the popular geometries in modern solid-state physics. This lattice is clearly periodic, but it is not a Bravais lattice *per se*, because its lattice sites can not be described with Eq. (1.1). Bravais lattice of the honeycomb lattice is constructed by connecting second neighbors, as shown in Fig. 1.1. The unit cell then contains two sites of the parent honeycomb lattice, one at the corner and one in the interior. This situation is known as a Bravais lattice *with basis*. Here, basis is the group of atoms contained by the unit cell. Of course, it is also possible to choose hexagon as the repetition unit of the honeycomb lattice. However, such a choice would introduce a disparity with other lattices, such as square lattice where the repetition unit is obviously a square. The advantage of Eq. (1.1) lies in the unified description of all periodic structures, so it is not surprising that Bravais lattice became the cornerstone of solid-state physics.

1.2. Close packing and structures of metals

A naive way of seeing crystals is arrays of atoms placed in the positions defined by Eq. (1.1). The most dense packing is achieved when atoms touch each other. Consider atom as a sphere and put such atoms onto a simple cubic lattice. Its lattice parameter should be twice the radius of the sphere, $a = 2r$. With one sphere per unit cell, the volume occupied by the sphere is $V_{\text{sphere}} = \frac{4}{3}\pi r^3 = \pi a^3/6$. On the other hand, the unit-cell volume is $V_{\text{cell}} = a^3$. The ratio of these two volumes is the *packing fraction*, $p = V_{\text{sphere}}/V_{\text{cell}}$, and amounts to only 52% for the simple

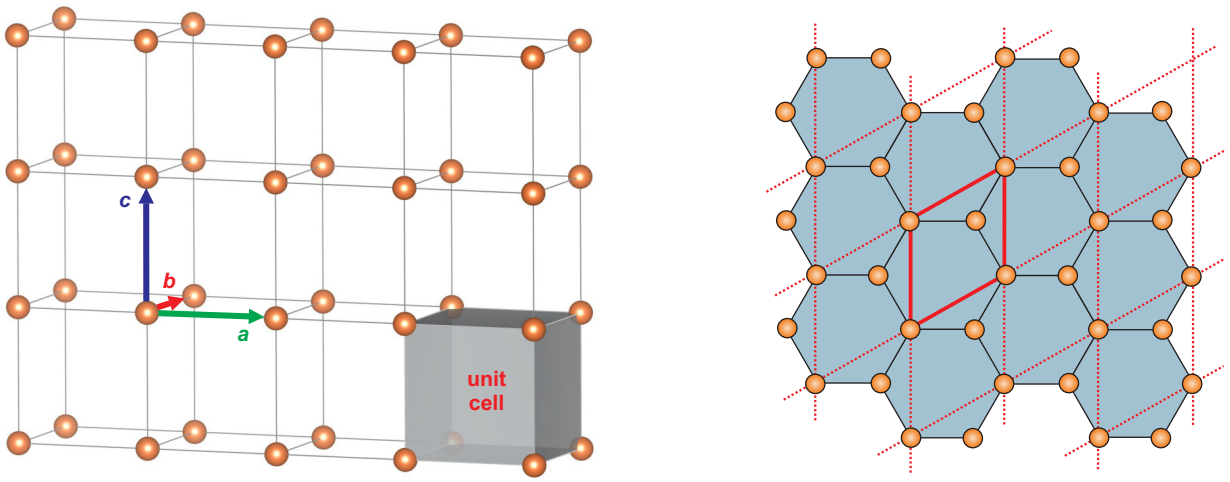

Figure 1.1: Left: Bravais lattice, lattice vectors, and unit cell. Right: honeycomb lattice is not a Bravais lattice *per se*; its Bravais lattice is indicated by the red lines, with two atoms per unit cell.

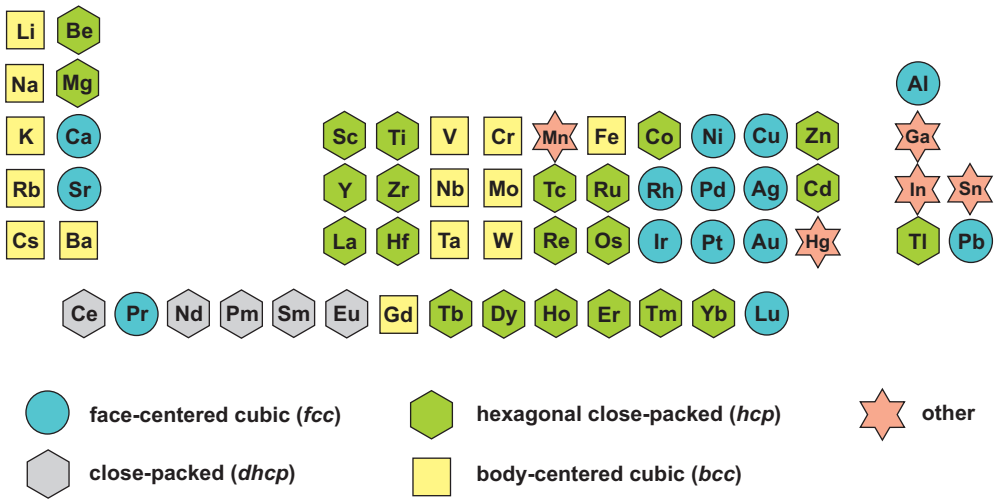

Figure 1.2: Structures of simple metals. *dhcp* is the double-hexagonal close-packing, ...ABACABAC...

cubic lattice. We can also introduce the *coordination number*, i.e., the number of neighboring atoms, which is as low as 6 in this case. Simple cubic lattice does not allow dense structures.

Finding a dense packing of spheres (better known as *close packing* in solid-state physics) is in fact a common mathematical problem. By solving it, or by using general intuition of putting together spherical objects like billiard balls, we know that each sphere can be surrounded by six other spheres, resulting in a close-packed honeycomb layer. The next layer should follow the dips formed by the first one. Different possible stackings give rise to a series of close-packed structures, including:

- ...ABABAB... (*hcp* or hexagonal close packing)
- ...ABCABC... (*ccp* or cubic close packing, or *fcc* = face-centered cubic structure)

These two structures are much denser than the simple cubic lattice, thanks to the coordination number of 12 (six neighbors in each layer, plus three neighbors in each of the two adjacent layers). They are in fact common for simple metals, which are well described by this packing concept because only one type of atoms is present in the crystal and because denser packing allows higher electron concentration, which is favorable for the metallic bonding. Fig. 1.2 shows that more than half of simple metals adopt either hcp or fcc structures. Most of the remaining metals form a bcc (body-centered cubic) structure, which is only slightly less dense than the close-packed ones.

lattice type	*packing fraction*	*coordination number*
simple cubic	0.52	6
body-centered cubic (bcc)	0.68	8
hexagonal close-packed (hcp)	0.74	12
face-centered cubic (fcc)	0.74	12

The choice between the bcc, fcc, and hcp structures for a given metal is far from trivial and depends on details of its band structure (Ch. **??**). Nevertheless, already at this point we can make a general prediction that bcc metals should transform into hcp or fcc structures on compression. This happens indeed in alkaline metals and also in iron that looses its magnetism upon transforming from bcc to hcp polymorph around 15 GPa (why denser structures are less likely to be magnetic is a separate and rather non-trivial question that will only be covered in the Advanced Solid-State Physics module).

1.3. Electron microscopy

Back in time researchers could only guess about lattice periodicity and packing. Nowadays it is possible to visualize the crystal lattice and even see individual atoms with the direct imaging done by electron microscopy. Electron microscopes are somewhat similar to common optical microscopes, but they use electrons as radiation with the much shorter wavelength, and of course they require a much more sophisticated system of electromagnetic lenses to direct and focus the electron beams.

Electron microscopes come in two main varieties:

- *transmission electron microscopes* (TEM) collect electrons on a detector behind the sample, just like an optical microscope does with visible light
- *scanning electron microscopes* (SEM) collect secondary electrons that are produced when electrons are scattered on the sample

SEM's are more compact, because one does not need a long separation between the sample and detector. They can also map a larger area by scanning the sample with the electron beam (hence the name). Concurrently, they lack in resolution. A typical instrument of this type has the resolution of about 10 nm and can be used for imaging microstructures but not individual atoms. By contrast, modern TEM's have the resolution of 1 Å. They can operate in different imaging modes and highlight heavy or light atoms, or map out chemical composition and even electronic states on the sub-nm scale.

Two points of concern when using electron microscopy are:

- small size of the probe; a region of only $20-30$ nm is probed in a single image taken with the atomic resolution. This problem is partially mitigated by STEM (scanning TEM), but even in this case only a tiniest fraction of the sample volume can be studied
- sample damage caused by the strong electron beam and high vacuum

Electron microscopy is the method of choice for studying defects and microstructures. When it comes to long-range-ordered crystals, electron microscopy plays a somewhat auxiliary role, while main information about the crystal structure comes from diffraction methods (Ch. 6).

2. Symmetry as the guiding principle

2.1. Symmetry operations

Long-range order of a crystal reflects its underlying symmetry. Most generally, *symmetry* of an object is a set of transformations that leave this object invariant. We will consider geometrical transformations that can be represented as

$$\text{symmetry operation} \;=\; \mathbb{R} \oplus \mathbf{t} \;=\; \begin{pmatrix} R_{xx} & R_{xy} & R_{xz} \\ R_{yx} & R_{yy} & R_{yz} \\ R_{zx} & R_{zy} & R_{zz} \end{pmatrix} \oplus \begin{pmatrix} t_x \\ t_y \\ t_z \end{pmatrix} \tag{2.1}$$

where $\mathbb{R}$ is a unitary transformation, such as rotation, and $\mathbf{t}$ is a translation in space by a given vector.

2.2. Translational symmetry: lattice centering

The simplest translational symmetry of a crystal is its periodicity. From Eq. (1.1) we know that $\mathbf{a}, \mathbf{b}, \mathbf{c}$ and their linear combinations are allowed translations, so all of them are symmetry operations of a crystal, as long as this crystal is periodic. Some other translations may be allowed too, leading to a classification of lattices by *lattice centering* into:

- *Primitive lattice* (P) has only $\mathbf{a}, \mathbf{b}, \mathbf{c}$ and their linear combinations as allowed translations
- *Face-centered lattice* (F) features additional translations $\mathbf{t} = \frac{1}{2}(\mathbf{a} \pm \mathbf{b}), \frac{1}{2}(\mathbf{a} \pm \mathbf{c}), \frac{1}{2}(\mathbf{b} \pm \mathbf{c})$ (half of the face diagonal for each face)
- *Body-centered lattice* (I) features additional translations $\mathbf{t} = \frac{1}{2}(\mathbf{a} \pm \mathbf{b} \pm \mathbf{c})$ (half of the body diagonals)
- *Base-centered lattice* (A, B, C) features additional translations by half of the face diagonal, but only for two faces out of six. For example, the C-centered lattice allows $\mathbf{t} = \frac{1}{2}(\mathbf{a} \pm \mathbf{b})$
- *Rhombohedral lattice* (R) features an additional translation by $\mathbf{t} = \frac{1}{3}(\mathbf{a}+\mathbf{b}+\mathbf{c})$ (one third of the body diagonal)

One could then ask why these additional vectors $\mathbf{t}$ are needed. Should they exist, lattice vectors can be re-defined as the shortest repetition vectors of the crystal, and every lattice will be primitive. True indeed, but some rotational symmetry may be lost on the way, as shown in Fig. 2.1. Therefore, in a centered lattice one distinguishes:

- *Primitive cell*, which is the repetition unit with the smallest volume defined by the shortest translations $\mathbf{a}_p$, $\mathbf{b}_p$, $\mathbf{c}_p$

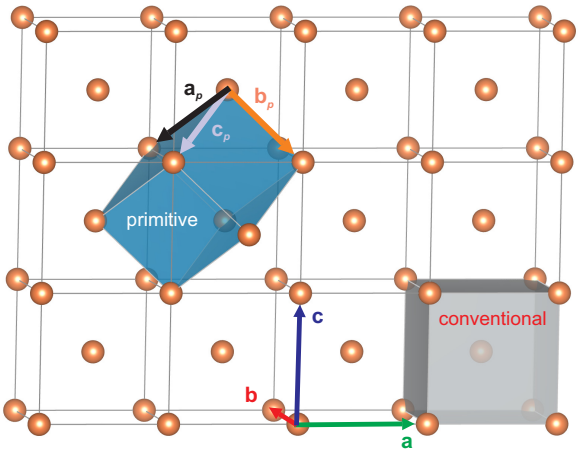

Figure 2.1: Conventional and primitive unit cells of the body-centered cubic lattice. The lattice angles of the primitive cell deviate from 90°, so it has a lower symmetry than the conventional cell. Note that $\mathbf{a}_p, \mathbf{b}_p, \mathbf{c}_p$ are also shorter than $\mathbf{a}, \mathbf{b}, \mathbf{c}$, hence the primitive cell has the twice smaller volume than the conventional one.

- *Conventional cell*, which is the smallest repetition unit of the highest symmetry defined by the lattice vectors $\mathbf{a}, \mathbf{b}, \mathbf{c}$

In a primitive lattice, both unit cells coincide. In a centered lattice, the volume of the primitive cell is twice (A, B, C, I), three times (R), or four times (F) smaller than the volume of the conventional unit cell.

From this point on, we will distinguish *lattice vectors* $\mathbf{a}, \mathbf{b}, \mathbf{c}$ that define the conventional unit cell, from *lattice translations* $\mathbf{t}$ that include $\mathbf{a}, \mathbf{b}, \mathbf{c}$ along with other vectors allowed by the lattice centering.

Lattice centering is an important part of describing crystal symmetry, but it may not have any immediate implications. We do not expect crystals with face-centered lattices to be distinct from the body-centered ones. However, in special cases, such as simple metals from Fig. 1.2, lattice centering determines the packing fraction and directly affects density of the crystal.

2.3. Rotational symmetry and birefringence

The p-fold *rotation axis* is defined as the rotation by $\varphi = 360°/p$. Here, p must be integer because applying the same operation several times should end up in the full 360° rotation. Rotation axes are labeled with numbers: two-fold rotation axis is 2, four-rold rotation axis is 4, etc. For a clockwise rotation, the corresponding transformation matrix is

$$\mathbb{R} = \begin{pmatrix} \cos\varphi & \sin\varphi & 0 \\ -\sin\varphi & \cos\varphi & 0 \\ 0 & 0 & 1 \end{pmatrix} \tag{2.2}$$

for a p-fold rotation axis parallel to z.

Rotation axes have some immediate ramifications. First, they impose constraints on lattice parameters. Consider a four-fold rotation axis along c. This symmetry operation transforms $\mathbf{a}$ into $\mathbf{b}$ and thus requires not only $a = b$, but also $\gamma = 90°$. Three of such axes render a crystal cubic!

Another ramification concerns crystal properties. A crystal with one 4-fold rotation axis shows distinct properties along this direction and in the plane perpendicular to it. This disparity is pretty obvious if we turn the crystal and measure its property along different directions. In fact, it can be seen even in a single experiment! Crystals refract light, and refractive index depends on the light polarization. Light polarized along the symmetry axis (i.e., the light with the electric field vector parallel to the symmetry axis of the crystal) and light polarized perpendicular to the symmetry axis feature different refractive indices, $n_\parallel$ and $n_\perp$, respectively. A non-polarized light is split by such a crystal into two distinct beams. This effect is known as *birefringence* ($\Delta n = n_\parallel - n_\perp$).

Historically, birefringence has been the very first tool used to identify crystal symmetries. It is still employed by geologists during field trips where advanced instruments are not available. It is also used technologically for a quick monitoring of product quality. Amorphous solids are normally isotropic and should not exhibit birefringence (for example, it's not seen in ordinary glass). However, strains lead to anisotropy and can be mapped out by shining a suitably polarized light on the sample. You can read more about it here.

2.4. Reflection and inversion symmetry

Eq. (2.2) covers only some of the unitary transformations. Two further important operations are *inversion center* (labeled $\bar{1}$ or -1) and *mirror plane* (m),

$$\mathbb{R}_{\text{inversion}} = \begin{pmatrix} -1 & 0 & 0 \\ 0 & -1 & 0 \\ 0 & 0 & -1 \end{pmatrix}, \qquad \mathbb{R}_{\text{reflection}} = \begin{pmatrix} 1 & 0 & 0 \\ 0 & 1 & 0 \\ 0 & 0 & -1 \end{pmatrix}, \tag{2.3}$$

where the latter describes a mirror plane perpendicular to z ($m \perp \mathbf{c}$). These symmetry elements can be combined with the rotation axes, namely, both can be present in the crystal at the same time.

The reflection and inversion symmetries also have important implications. They determine polarity and chirality of the crystal. We will get back to this in Ch. 3 after we learn how individual symmetry elements build up a symmetry group.

2.5. Neumann's principle

A general and very intuitive principle commonly attributed to Neumann is that *properties of a crystal should be invariant under its symmetry operations*. Neumann's principle is usually invoked in its mathematical form, which states that any tensor property $\boldsymbol{\sigma}$ should follow

$$\boldsymbol{\sigma} = \mathbb{R}^{-1}\boldsymbol{\sigma}\mathbb{R}. \tag{2.4}$$

Consider linear-response properties, such as conductivity $\boldsymbol{\sigma}$ defined by Ohm's law $\boldsymbol{j} = \boldsymbol{\sigma}\,\mathbf{E}$ ($\boldsymbol{j}$ is electric current density and $\mathbf{E}$ is electric field) or permittivity $\boldsymbol{\varepsilon}$ defined by $\mathbf{P} = (\boldsymbol{\varepsilon} - 1)\varepsilon_0\mathbf{E}$ ($\mathbf{P}$ is electric polarization). Both $\boldsymbol{\sigma}$ and $\boldsymbol{\varepsilon}$ are second-rank tensors because electric field applied along one direction causes a response, polarization or current, along all three directions of the crystal. We express this idea by writing

$$j_\alpha = \sigma_{\alpha\beta}E_\beta \tag{2.5}$$

and implying that conductivity has the general form of

$$\boldsymbol{\sigma} = \begin{pmatrix} \sigma_{xx} & \sigma_{xy} & \sigma_{xz} \\ \sigma_{yx} & \sigma_{yy} & \sigma_{yz} \\ \sigma_{zx} & \sigma_{zy} & \sigma_{zz} \end{pmatrix} \tag{2.6}$$

with up to 9 independent components.

Such tensors are usually symmetric, $\sigma_{\alpha\beta} = \sigma_{\beta\alpha}$. Their symmetry is rooted in some fundamental physical principles. For thermodynamic (equilibrium) properties it follows simply from their definition via change of free energy in the applied field,

$$dG = -S\,dT + V\,dp - \mathbf{P}\,d\mathbf{E} \;\Rightarrow\; \mathbf{P} = -\left(\frac{\partial G}{\partial \mathbf{E}}\right)_{T,p}. \tag{2.7}$$

Permittivity is then related to the second derivative of G with respect to $\mathbf{E}$, and mixed derivatives must be equal,

$$\frac{\partial^2 G}{\partial E_\alpha \partial E_\beta} = \frac{\partial^2 G}{\partial E_\beta \partial E_\alpha} \;\Rightarrow\; \varepsilon_{\alpha\beta} = \varepsilon_{\beta\alpha}. \tag{2.8}$$

A similar statement for transport properties is known as Onsager reciprocal relations. Without going into details we only mention here that these relations need to be amended in the presence of a magnetic field where conductivity tensor becomes antisymmetric (more on this in Ch. **??**).

Symmetry of the tensor reduces the number of independent components from 9 to 6. Additional constraints can be derived from crystal symmetry using Eq. (2.4). For example, consider the 4-fold rotation axis parallel to z. According to Eq. (2.2), it leads to the transformation $(x, y, z) \to (y, -x, z)$ that converts $\boldsymbol{\sigma}$ into an equivalent tensor $\boldsymbol{\sigma}'$,

$$\boldsymbol{\sigma}' = \begin{pmatrix} \sigma_{yy} & -\sigma_{yx} & \sigma_{yz} \\ -\sigma_{xy} & \sigma_{xx} & -\sigma_{xz} \\ \sigma_{zy} & -\sigma_{zx} & \sigma_{zz} \end{pmatrix} \quad \text{vs.} \quad \boldsymbol{\sigma} = \begin{pmatrix} \sigma_{xx} & \sigma_{xy} & \sigma_{xz} \\ \sigma_{yx} & \sigma_{yy} & \sigma_{yz} \\ \sigma_{zx} & \sigma_{zy} & \sigma_{zz} \end{pmatrix}. \tag{2.9}$$

The tensor components should be pairwise equal, so $\sigma_{yy} = \sigma_{xx}$, whereas $-\sigma_{yx} = \sigma_{xy}$. For a symmetric tensor it means that all off-diagonal components vanish, leading to the final form of

$$\boldsymbol{\sigma} = \begin{pmatrix} \sigma_{xx} & 0 & 0 \\ 0 & \sigma_{xx} & 0 \\ 0 & 0 & \sigma_{zz} \end{pmatrix} \tag{2.10}$$

for a crystal with the 4-fold symmetry axis.

Tensor form for a given crystal symmetry can be checked on the Bilbao server.

2.6. Rotation vs. periodicity

Different symmetry operations have been friends until now, but they can be foes too. Specifically, not every kind of rotational symmetry is compatible with periodicity of the lattice. One can show that only 2-fold, 3-fold, 4-fold, and 6-fold rotations do not forbid periodicity in two and three dimensions and can be thus present in periodic crystals. This statement is known as crystallographic restriction theorem. Its mathematical proof can be found here.

Forbidden symmetries are not entirely impossible. For example, one may consider a crystal with the 5-fold symmetry and, therefore, without periodicity. Such crystals have been discovered in 1980's and dubbed *quasicrystals*. They are typically metallic and combine several chemical elements in rather weird proportions like $Al_{65}Cu_{20}Fe_{15}$. They serve as examples of aperiodic crystals.

3. Systematics of crystals: symmetry groups

3.1. Point symmetry operations

Only a few local (point) symmetry operations $\mathbb{R}$ are compatible with periodicity. Every periodic crystal can be then assigned to one or another symmetry group that comprises a subset of the following symmetry elements:

- Rotation axes: $2, 3, 4, 6$ (C_2, C_3, C_4, C_6)
- Inversion center: $\bar{1}$ (i)
- Mirror plane: m (σ_v, σ_h)
- Rotoinversion axes: $\bar{3}$, $\bar{4}$, $\bar{6}$

Here, we use labels in the international (Hermann-Mauguin) notation, which is common in crystallography. The symbols in brackets are Schönflies notation favored by spectroscopists.

The last element, *rotoinversion axes*, has not been discussed yet and requires a further comment. This symmetry element is a rotation followed by inversion,

$$\mathbb{R}_{\bar{n}} = \begin{pmatrix} -\cos\varphi & -\sin\varphi & 0 \\ \sin\varphi & -\cos\varphi & 0 \\ 0 & 0 & -1 \end{pmatrix} \tag{3.1}$$

The inversion center $\bar{1}$ is in fact the end member of this series, because it combines inversion with the 1-fold rotation. Using Eqs. (2.2) and (2.3), one can verify that $\bar{2} = m$. Three other rotoinversion axes are independent symmetry elements, which are needed to describe special situations, such as the symmetry of a tetrahedron $(\bar{4})$.

No Schönflies symbols for rotoinversion axes exist, because a different symmetry element, *rotation-reflection axes* (S_n), is considered in this case. They are quite similar to $\bar{n}$, but rotation is followed by a mirror-plane reflection. This operation is also known as an *improper rotation*,

$$\mathbb{R}_{S_n} = \begin{pmatrix} \cos\varphi & \sin\varphi & 0 \\ -\sin\varphi & \cos\varphi & 0 \\ 0 & 0 & -1 \end{pmatrix} \tag{3.2}$$

assuming $S_n \parallel z$. Simple algebra shows that $\bar{3} = S_6$, $\bar{6} = S_3$, and $\bar{4} = S_4$, whereas $S_2 = \bar{1}$ and $S_1 = m$, so we end up with exactly the same symmetry operations and an unnecessarily confusing notation.

3.2. Point groups and crystal classes. Polarity

A combination of symmetry elements constitutes a *symmetry group*. Here, group is used in mathematical sense, as a closed set of elements with an operation that transforms them into each other. For example, a two-fold rotation axis and a mirror plane perpendicular to it generate the symmetry group (Fig. 3.1):

$$2/m = \{\, 1, 2, m, \bar{1} \,\}. \tag{3.3}$$

Repeated application of the two-fold rotation leads to the unitary operation, $2 \otimes 2 = 1$. The same is true for the mirror plane, $m \otimes m = 1$. Finally, 2 followed by m results in the inversion center $\bar{1}$.

Another example: a point group composed of three mutually orthogonal mirror planes perpendicular to **a**, **b**, and **c** (Fig. 3.1). A consecutive application of m_a and m_b leads to the coordinate transformation $x, y, z \longrightarrow \bar{x}, \bar{y}, z$, so it is equivalent to a two-fold rotation axis

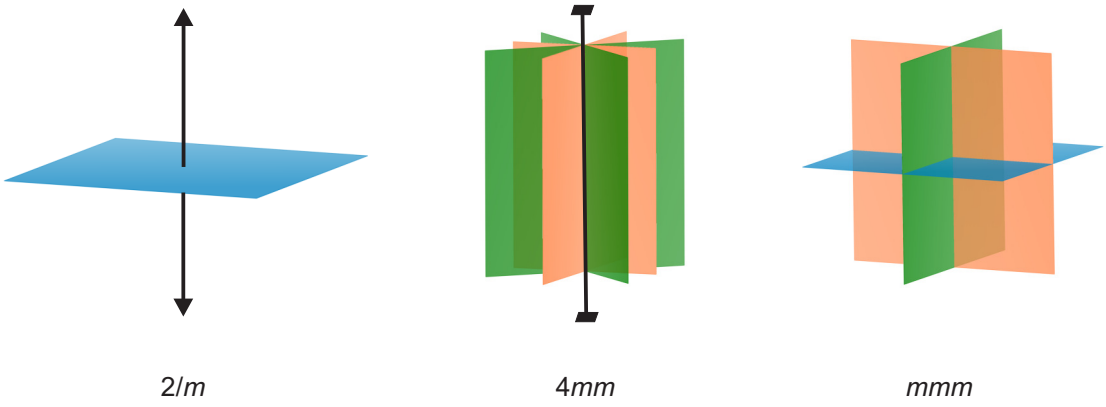

Figure 3.1: Examples of point groups of symmetry.

along **c**. Each pair of planes generates a rotation axis, but we don't need to list them all, and the point group is labeled simply as mmm. It features eight symmetry elements,

$$mmm = \{\, 1, 2_a, 2_b, 2_c, m_a, m_b, m_c, \bar{1}\,\}\,. \tag{3.4}$$

Since one symmetry element can be obtained from a few others, it is customary to label the symmetry group by its main generators, similar to the examples above. One usually chooses rotation axis of the highest order and then symmetry elements perpendicular to it. Consider the following examples:

- $4/m$ is the four-fold rotation along **c** and the mirror plane perpendicular to **c**.
- $4mm$ is the four-fold rotation along **c**, the mirror planes perpendicular to **a** and **b**, and the mirror planes perpendicular to $\mathbf{a} \pm \mathbf{b}$. The absence of / means that no mirror plane perpendicular to **c** occurs. Moreover, the **a** and **b** directions are equivalent (orange planes in Fig. 3.1), so they are mentioned only once, while the second m stands for the mirror planes, which are perpendicular to the ab-diagonals (green).

There are altogether 32 *point groups* formed by the symmetry operations from Ch. 3.1. The full list can be found on Wikipedia along with an explanation of the Schönflies symbols of point groups that we will not consider here. Every point group defines its own *crystal class*, a family of crystals with the similar shape that reflects the underlying symmetry of the crystal structure.

The relation between the crystal class and crystal shape is most useful in mineralogy. Synthetic crystals can be grown in different shapes, and they are often cut to a custom shape as required by the experiments. The point symmetry remains important, though, because it determines whether or not the crystal is polar. *Polar direction* is defined as the direction that stays invariant under all symmetry operations of the system. Crystal or molecule with at least one polar direction are capable of having dipole moment and electric polarization, which is important for ferroelectric and pyroelectric properties. Inversion centers and rotoinversion axes obviously forbid polarity. Examples of *polar* symmetries are $4mm$ and $3m$, examples of *non-polar* symmetries are $4/m$ and $3\,2$.

3.3. Crystal systems

32 points groups are hard to remember, and only crystallographers know them all (simply from experience and not from hard learning), but it is useful to be familiar with seven *crystal systems* that are distinguished by symmetry constraints imposed on the lattice parameters:

Cubic	$a = b = c$, $\alpha = \beta = \gamma = 90°$	$m\bar{3}m$, $\bar{4}3m$, 432, $m\bar{3}$, 23
Tetragonal	$a = b \neq c$, $\alpha = \beta = \gamma = 90°$	4, $4mm$, $4/m$, $4/mmm$, $\bar{4}$, 422, $\bar{4}2m$
Orthorhombic	$a \neq b \neq c$, $\alpha = \beta = \gamma = 90°$	222, $mm2$, mmm
Hexagonal	$a = b \neq c$, $\alpha = \beta = 90°$, $\gamma = 120°$	6, $6/m$, $6mm$, $6/mmm$, $\bar{6}$, 622, $\bar{6}m2$
Trigonal	$a = b \neq c$, $\alpha = \beta = 90°$, $\gamma = 120°$	3, $3m$, $\bar{3}$, $\bar{3}m$, 32
Monoclinic	$a \neq b \neq c$, $\alpha \neq \gamma \neq 90°$, $\beta = 90°$	2, m, $2/m$
Triclinic	$a \neq b \neq c$, $\alpha \neq \beta \neq \gamma \neq 90°$	$1, \bar{1}$

Crystal system defines the form of tensor properties according to Neumann's principle, as explained in Ch. 2.5. The knowledge of the crystal system is also important for constructing reciprocal lattice and analyzing diffraction experiments, as we will see in Ch. 4 and 5.

Crystal system can be combined with the lattice centering from Ch. 2.2. Back then, we mentioned that centering only makes sense when the conventional unit cell has a higher symmetry than the primitive cell. Otherwise, lattice vectors could be re-defined without loss of symmetry. Indeed, a centered triclinic lattice is redundant, because its unit cell can always be reduced. On the other hand, both face and body-centering occur for cubic and some other crystal systems where symmetry elements would be lost otherwise. Combining crystal systems and lattice centering gives rise to *14 Bravais lattices* that can be encountered in periodic crystals.

3.4. Open symmetry elements

Only point symmetry operations have been considered so far. Crystals also feature translational symmetry, and they are allowed to have combined symmetry elements that contain both local transformations and translations within one operation in the sense of Eq. (2.1). Such symmetry elements are called *open* because they generate an infinite array out of a single atom.

Importantly, open symmetry elements can only occur in crystals, so they are always accompanied by pure translations (Ch. 2.2) and should be compatible with periodicity. Repeated application of an open symmetry element leads to a simple shift of an atom without any reflection or rotation. This shift should match one of the lattice translations that have been defined in Ch. 2.2.

Two types of open symmetry elements should be introduced: glide plane and screw axis. *Glide plane* is a mirror reflection followed by a shift $\mathbf{t}'$. The label of the glide plane indicates the shift direction:

- a, b, c involve the shift by half of the corresponding lattice vector; for example, $\mathbf{t}' = \mathbf{a}/2$ in the case a
- n involves the shift by half of the face diagonal; for example, $\mathbf{t}' = (\mathbf{a} \pm \mathbf{b})/2$
- d involves the shift by one quarter of the face or body diagonal; for example, $\mathbf{t}' = (\mathbf{a} \pm \mathbf{b})/4$; it only occurs in the presence of lattice centering, because the shift by $2\,\mathbf{t}'$ should be an allowed lattice translation

The shift direction is always parallel to the plane. For example, an a glide plane can't be perpendicular to the lattice vector $\mathbf{a}$.[2] Otherwise, repeated application of the glide plane would generate a new translational symmetry along a, which is incompatible with the lattice translations.

Screw axis is a rotation followed by a shift of $\mathbf{t}'$ along this axis. Here, the shift direction is fixed, but the length of $\mathbf{t}'$ should match the order of rotation. The screw axis $n_p \parallel \mathbf{c}$ involves the rotation by $360°/n$ followed by the shift of $\mathbf{t}' = \frac{p}{n}\,\mathbf{c}$. For example:

[2] Note that we have to distinguish italicized symbols (a), which are used for the glide planes, from bold symbols ($\mathbf{a}$) used for vectors.

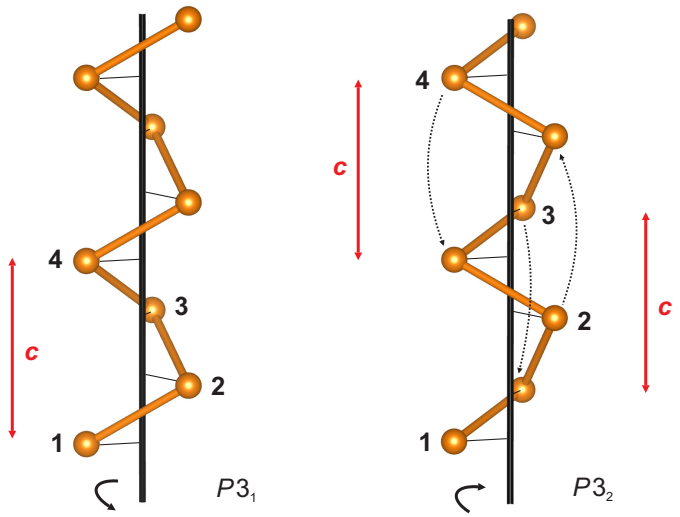

Figure 3.2: Helical chains formed by the 3_1 and 3_2 screw axes in elemental tellurium. The numbers **1-2-3-4** show the consecutive action of the symmetry operator. In the case of 3_2, the missing atoms are added through the regular lattice translation by **c**.

- 3_1 is the 120° rotation followed by a shift of $\mathbf{c}/3$
- 4_2 is the 90° rotation followed by a shift of $\mathbf{c}/2$

3.5. Chirality

Screw axes impart their sense of rotation to the atomic arrangement and, therefore, to the crystal as a whole. For example 3_1 and 3_2 produce similar helical chains with the counter-clockwise and clockwise rotations, respectively (Fig. 3.2). It is an example of chirality.

More generally, *chirality* is defined as the property of an object not to match its mirror image. Mirror-plane symmetry renders an object non-chiral because the object does not change under this operation at all. On the other hand, any symmetry group that does not contain mirror operations (nor it contains inversion centers and rotoinversion axes, which are equivalent to the rotation-reflection axes) is chiral. Examples of chiral point groups are 2 2 2 and 3 2. Note that some symmetry groups are polar and non-chiral or chiral and non-polar. Both polarity and chirality are rooted in the crystal symmetry, but different aspects of the symmetry are relevant in each case.

Chiral objects are interesting because they exist in (at least) two forms, known as left and right *enantiomers* (for molecules) and *enantiomorphs* (for crystals). These forms are almost indistinguishable, yet they may show drastically different properties. For example, many of the aminoacids, carbohydrates, and other biologically relevant molecules are chiral. Only one enantiomer is usually present in nature, and this choice of chirality has tremendous repercussions for biological systems.

3.6. Circular birefringence and dichroism

Chirality has direct implications for optical properties. Previously (Ch. 2.3), we discussed birefringence as the different refraction of light depending on its polarization relative to the crystal directions. A counterpart of this effect is *dichroism*, the different absorption of light depending on its polarization.[3] Crystals with a suitable symmetry may change color on rotation when illuminated by the linearly polarized light. This is *linear dichroism* (different absorption of linearly polarized light) also known as pleochroism in the context of minerals.

A similar effect in chiral crystals is known as *circual birefringence* and *circular dichroism*. Here, one uses left- and right- circularly polarized light and observes their different refraction

[3]More generally, birefringence and dichroism describe anisotropy for the real and imaginary parts of the refractive index, respectively. See also Ch. 12.1.

or absorption. Circular birefringence is the manifestation of an *optical rotation*. The polarization direction turns when light goes through a chiral material. This has been the earliest experimental tool for identifying chirality. It can be observed in very common systems, such as crystalline sugar and sugar syrup.

3.7. Space groups

Full symmetry of the crystal is defined by its:

- lattice centering that contains all translations allowed in this crystal (Ch. 2.2)
- point symmetry elements (Ch. 3.1)
- open symmetry elements (Ch. 3.4)

The combination of the three makes a *space group*. Space groups are labeled by four symbols: the first one indicates lattice centering, while the three others stand for symmetry elements along three nonequivalent directions. For example, $Pnma$ means:

- primitive lattice
- n glide plane perpendicular to **a**
- mirror plane (m) perpendicular to **b**
- a glide plane perpendicular to **c**

Absent symmetry elements are usually not written. For example, $P2/m = P\,1\,2/m\,1$. On the other hand, $P\,4_2/m\,b\,c$ means

- 4_2 screw axis along **c** and a mirror plane (m) perpendicular to **c**
- b glide plane perpendicular to **a** (and, respectively, a glide plane perpendicular to **b**)
- c glide planes perpendicular to $\mathbf{a} \pm \mathbf{b}$

(check again Ch. 3.2 for the choice of directions in the 4-fold symmetric case).

An exhaustive list of *230 space groups* can be found on the Bilbao Crystallographic Server and in International Tables for Crystallography.[4] While 230 may look like a huge number, it still means that the number of possible symmetries is finite, so it is possible to go through each of them when necessary. Many of the interesting crystal properties become possible for selected symmetries only. Then the classification of crystals by their space groups helps one to identify those specific materials where the property of interest is likely to appear. This approach has been common in many recent studies, for example here.[5]

The crystal class is determined by both point and open symmetry elements of the space group, because open symmetry elements have the same effect on lattice symmetry as the point ones. For example, $Pnma$ belongs to the mmm crystal class and orthorhombic crystal system. $P4_2/mbc$ belongs to the $4/mmm$ crystal class and tetragonal crystal system. Both space groups are non-polar and non-chiral.

One tricky thing about space groups is that their different settings are usually possible. For example, $Pmmn$, $Pnmm$, and $Pmnm$ are all the same space group with the different choices of $\mathbf{a}, \mathbf{b}, \mathbf{c}$. Likewise, $P2/a$ and $P2/c$ are the same space group, with the **a** and **c** axes swapped. Such an ambiguity is unavoidable, but it has been mitigated by creating a catalog of space groups in their standard settings, again at the Bilbao server and in related sources. Each space group has got a unique number, which is often supplied in publications along with the space

[4] Many of the universities, including Leipzig, do not have access to this book. Fortunately, symmetry diagrams for many of the space groups can be also obtained free of charge from the The Fascination of Crystals and Symmetry website by Frank Hoffmann.

[5] Beware that you will need a quite advanced knowledge to understand the content of this paper.

group symbol. Crystalloghers have also done a great job in enforcing standard settings and standard notations for the crystal symmetry. You can take a peek into their very systematic and perfectly organized world by visiting the website of International Union of Crystallography with its own dictionary, teaching pamphlets, and a lot more.

4. Unpacking the crystal structure

4.1. Atomic coordinates and Wyckoff positions

Atomic positions in a crystal are defined as fractions of lattice translations,

$$\mathbf{r} = x\mathbf{a} + y\mathbf{b} + z\mathbf{c}, \tag{4.1}$$

where x, y, z are *fractional (crystallographic) coordinates*. Their convenience in solid-state physics context will become clear soon (Ch. 5). On the other hand, evaluation of interatomic distances using x, y, z does become problematic when lattice angles deviate from 90°. Whereas distances can be still calculated by hand, it is usually more practical to use dedicated software like VESTA that not only draws crystal structures but also gauges distances between the atoms and even measures bond angles. For atoms within the unit cell, $0 \leq x, y, z < 1$. Any other atom can be obtained via lattice translations.

Let an atom be placed at a position (x, y, z). Without symmetry, this atom may feel rather lonely, but a symmetry element will typically generate counterparts of an atom. For example, inversion center at $(0, 0, 0)$ creates a counterpart at $(\bar{x}, \bar{y}, \bar{z})$.[6] A two-fold rotation axis, $2 \parallel \mathbf{a}$, creates a counterpart at $(x, \bar{y}, \bar{z})$ and so on. In this way, symmetry elements generate a *Wyckoff position*.

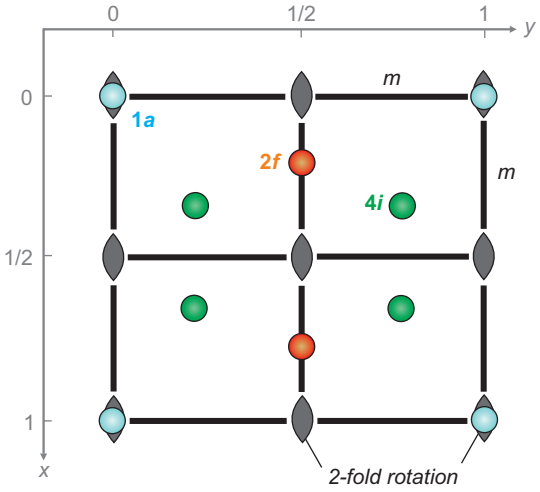

Figure 4.1: Selected Wyckoff positions of the space group $Pmm2$ (No. 25). $4i$ is the general position not lying on any symmetry element. $2f$ and $1a$ are special positions with the lower multiplicity. In this figure, we used some standard notation of the symmetry diagrams: solid lines show the mirror planes, whereas gray pointed ovals are the two-fold rotation axes. You can find more of the symbols here.

These Wyckoff positions can be general or special. A *general* Wyckoff position does not lie on any point symmetry element and shows the highest multiplicity allowed by the given space group. A *special* Wyckoff position lies on at least one point symmetry element, which then does not act on this atom, resulting in a lower multiplicity. For example, the general position in the space group $Pmm2$ has the multiplicity of 4; it is labeled $4i$. By contrast, the position $(0, 0, z)$ on the two-fold rotation axis has the multiplicity of 1 (it is labeled $1a$) because it stays invariant under all symmetry operations (Fig. 4.1).

Wyckoff positions have two implications. First, they help us to make the description of crystal structures more systematic. Lists of possible Wyckoff positions are available for every space group (again, on the Bilbao server or in the International Tables for Crystallography). Second, the distribution of atoms over different Wyckoff positions has ramifications for crystal properties, such as the type of phonon modes and their response in infrared and Raman experiments. We will briefly touch on this issue in Ch. 12. You can also learn more by trying the SAM utility at the Bilbao server.

[6] Crystallographers use bars to indicate minus sign in front of the coordinate.

4.2. Crystal structure

The structure of a given crystal is described by several elements:

- lattice parameters: a, b, c and α, β, γ
- symmetry (space group) symbol
- list of Wyckoff positions occupied by atoms, with the corresponding coordinates: x_j, y_j, z_j

You will almost never see the full list of atoms in the unit cell. Only the Wyckoff positions (i.e., positions unrelated by symmetry) will be given. Other atoms can be generated using symmetry elements.

Let's address several beginners' questions about crystal structures:

Where to find crystal structures? In databases that together contain over a million of crystal structures that have been determined experimentally. You can use Crystallography Open Database (free), Karlsruhe database or ICSD (commercial, inorganic compounds), and Cambridge Structural Database or CSD (commercial, organic compounds). Each of these databases contains the so-called cif-files that summarize structural information in a common format.

How to read crystal structures? Experts can learn a lot by reading the cif-file as plain text. However, most people will find it much easier to draw the crystal structure using software like VESTA. Then you immediately see all atoms, their positions relative to the unit cell and lattice translations, etc.

How to understand crystal structures? The answer to this question depends on the information that you seek to obtain. There are generally three ways of thinking about crystal structures, sometimes they are called structural models:

- *close packing*, works for relatively simple compounds, such as monoatomic crystals discussed in Ch. 1. We will see some further applications in the ionic crystals too (Ch. 7).
- *ball-and-stick* means that you connect atoms, which are sufficiently close to each other, and indicate chemical bonds. In this way, one finds connectivity of the crystal, whether it is built of molecules, chains, layers... This approach is most fruitful in covalent and van der Waals crystals (Ch. 8).
- *polyhedral* means that you connect an atom to its neighbors and treat the resulting unit as a rigid body. Then you analyze connectivity of such polyhedra. This approach is especially useful in more complex ionic crystals that can not be described as closed-packed structures.

4.3. Bragg's law

At first glance, there is not much more in a crystal than what we already considered: the atoms and their exact positions in space that can be extracted from Wyckoff positions with the use of lattice parameters and symmetry. However, we can also see this in a different light when shining light (with a properly chosen photon energy) on a crystal. In fact, most of the information about the crystal structure comes from scattering experiments where radiation with the short wavelength ($\lambda \sim 1$ Å in order to match the typical interatomic distances) is used. The simplest model of this scattering is given by Bragg's law.

Consider atomic planes separated by a distance d from each other (Fig. 4.2). The waves reflected by two adjacent planes accumulate the path difference of $2d \sin\theta$ where θ is the angle between the incident beam and the atomic plane. These waves interfere constructively when the path difference equals an integer number of wavelengths (m), leading to the simple condition

$$2d \sin\theta = m\lambda \tag{4.2}$$

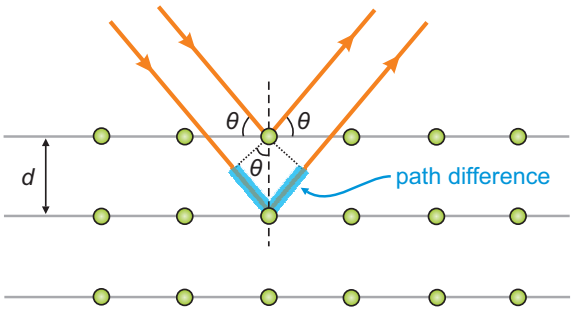

Figure 4.2: Bragg's law. Reflection of waves from parallel atomic planes gives rise to a constructive interference when the path difference is equal to an integer number of wavelengths. Experimentally, the angle 2θ between the incident and scattered waves is measured.

known as *Bragg's law*. It is customary to choose $m = 1$. Higher-order interference maxima may occur too, but we don't need to take them into account. In Ch. 5.3 we will see that these $m \neq 1$ maxima are in fact due to the $m = 1$ scattering but from different planes.

Bragg's law shows that by scattering waves such as x-rays on a crystal, one expects to see a series of intensity maxima known as *Bragg peaks* or simply *reflections*. Experimentally, the angle θ can not be measured, but the angle 2θ between the incident and scattered wave is easy to monitor. The 2θ positions of the Bragg peaks correspond to the distances d that contain information on the periodicity of the crystal. It is the basics of crystal structure determination, although by no means a complete procedure yet, as we will see in the following.

4.4. Scattering experiments and x-ray diffraction

The setup described by Bragg's law is an example of a scattering experiment. One generally distinguishes

- *elastic scattering* where the scattered beam has the same energy as the incident beam
- *inelastic scattering* where some energy is exchanged between the incident beam and the crystal

Elastic scattering is resolved in the angle 2θ. When Bragg peaks in the sense of Eq. (4.2) are observed, this experiment is called *diffraction*. Inelastic scattering can be resolved in both angle θ and energy transfer $\mathcal{E}$. This experiment is in fact similar to spectroscopy, although spectroscopy is a somewhat broader term that also includes experiments that are done at the fixed scattering angle and resolved in energy, only.

Scattering experiments can be done with any kind of waves. We will see such examples later in these lecture notes, but for now our favorite type will be x-rays because their wavelength is matched to the typical interatomic distances and lattice parameters. Other types of radiation can be neutrons and electrons, as we will see in Ch. 6.

X-ray diffraction, better known as *XRD*, is one of the most common experimental tools in solid-state research. It is essentially the scattering of monochromatic x-rays (photons with the single wavelength λ) on a crystalline sample. The scattered radiation is collected by a detector, and the angle 2θ between the incident and scattered beams is measured. A diffraction pattern with a series of Bragg peaks is recorded. The positions and intensities[7] of the Bragg peaks can be used for:

- identifying the sample and identifying different chemical compounds in mixed, multi-phase samples; each crystal structure gives rise to a unique series of Bragg peaks that serves as a fingerprint of this structure and underlying chemical compound.
- determining orientation of a crystal surface or a thin film
- resolving the crystal structure (more on this in Ch. 6)

[7] The role of the intensities will become clear in Ch. 6

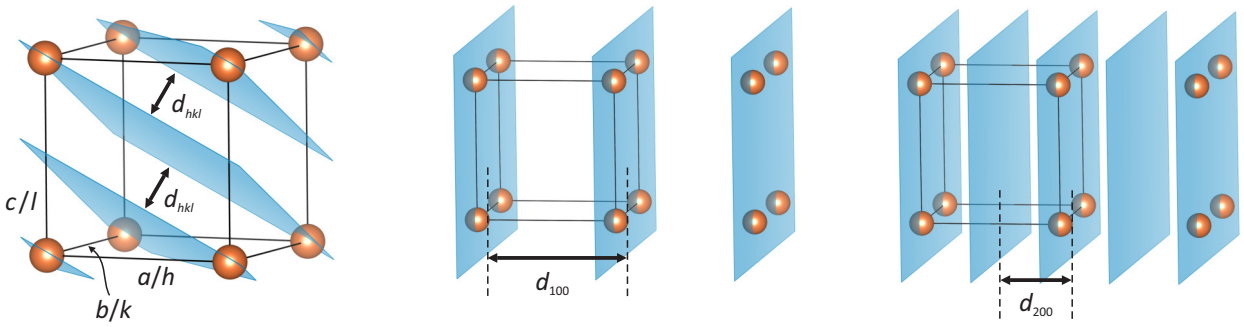

Figure 4.3: Left: definition of Miller indices h, k, l. The leftmost plane goes through the origin. An adjacent plane crosses the lattice vectors $\mathbf{a}, \mathbf{b}, \mathbf{c}$ at $d_a = a/h$, $d_b = b/k$, and $d_c = c/l$. The distance between the planes is d_{hkl}. Middle and right: the (200) planes are similar to the (100) planes but show a twice smaller spacing.

XRD is a much more versatile technique compared to electron microscopy (Ch. 1.3). It does not destroy the sample and does not require high vacuum. It is compatible with different sample environments and can be performed in a broad range of temperatures, pressures, electric and magnetic fields.

4.5. Lattice planes and Miller indices

The concept of atomic or *lattice planes* used in Bragg's law requires their proper classification. Importantly, in the derivation of Bragg's law one uses not a single lattice plane, but a series of periodically spaced planes of the whole crystal. Consider now two of these planes, the one that goes through origin and the plane adjacent to it. The latter crosses lattice vectors $\mathbf{a}, \mathbf{b}, \mathbf{c}$ at the positions d_a, d_b, d_c away from the origin (Fig. 4.3). Then *Miller indices* h, k, l for this family of atomic planes are defined as

$$h = a/d_a, \qquad k = b/d_b, \qquad l = c/d_c. \tag{4.3}$$

The Miller index of zero means that the lattice plane never crosses the respective axis, i.e., it is parallel to this axis. Three faces of the unit cell will then have indices of (100), (010), and (001). Increasing the Miller indices shortens the spacing between the planes. For example, (200) are the same lattice planes as (100), but with the twice shorter spacing (Fig. 4.3).

The Miller indices must be integer to comply with periodicity of the lattice. Later we will come to see that they also describe a position in the reciprocal space and can be arbitrary in this sense. However, only integer values of h, k, l describe something that matches periodicity of the crystal.

The Miller indices can be used to determine the d value in Bragg's law. For a crystal with $\alpha = \beta = \gamma = 90°$,

$$\frac{1}{d_{hkl}^2} = \frac{h^2}{a^2} + \frac{k^2}{b^2} + \frac{l^2}{c^2}. \tag{4.4}$$

We will prove this relation shortly (Ch. 5.3). For now let's explain how the actual experiment works. An XRD measurement returns a set of peak positions θ_i that can be re-calculated into d_i's using Bragg's law. Then one has to find the values of $a, b, c, \alpha, \beta, \gamma$ such that every d_i is described by some integer values of h, k, l. This procedure is known as *indexing* of the Bragg peaks. A successful indexing returns lattice parameters of the crystal.

4.6. Crystal faces and crystal directions

It should be clear from the above that crystal faces (and, consequently, surfaces) are labeled with the same Miller indices h, k, l. Here, one considers a single plane only, so there will be no difference between (100), (200), (300), and so on, hence the smallest indices are always used.

The notation of lattice planes and crystal faces should not be confused with the notation of crystal directions, even though three integer numbers u, v, w are also involved in this case,

$$\mathbf{R}_{[u\,v\,w]} = u\,\mathbf{a} + v\,\mathbf{b} + w\,\mathbf{c}. \tag{4.5}$$

In simple cases, these vectors $\mathbf{R}$ are perpendicular to the lattice planes with the same indices. For example, viewing a cubic crystal along the [100] direction means that you look at the (100) face of the cube. However, this is not true in general. We will see very soon that the h, k, l values define a vector in the reciprocal space, whereas Eq. (4.5) corresponds to a real-space direction. Note also the different type of brackets used for the (lattice planes) vs. [crystal directions].

5. Spaces of crystallography: Reciprocal lattice

5.1. Laue condition

Bragg's law is so simple that it does not describe all features of the scattering process. It does not account for the presence of different atoms, nor for the different reflection intensities, and it treats atomic planes as simple mirrors that reflect the incident beam in one direction. A more realistic description has been proposed by Laue who considered interference of waves scattered on two different atoms inside the crystals.

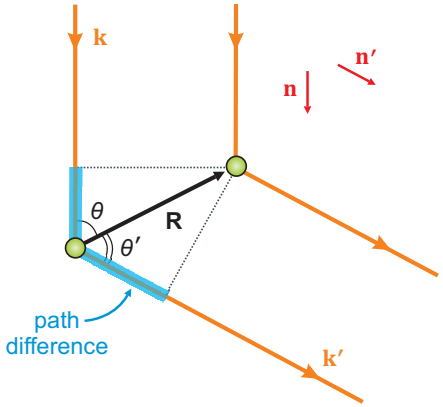

Figure 5.1: Laue condition of the constructive interference. The waves scattered by two atoms, which are separated by the lattice vector $\mathbf{R}$, acquire a path difference that should be a multiple of the wavelength λ. The unitary vectors $\mathbf{n}$ and $\mathbf{n}'$ show the directions of $\mathbf{k}$ and $\mathbf{k}'$, the propagation vectors of the incident and scattered waves, respectively.

Without loss of generality, we consider $\mathbf{k}$ and $\mathbf{k}'$, the propagation vectors of the incident and scattered waves, respectively. If two atoms are separated by a vector $\mathbf{R}$, the path difference between the two scattered waves becomes (Fig. 5.1)

$$R\cos\theta + R\cos\theta' = \mathbf{R}\,(\mathbf{n}' - \mathbf{n}) \tag{5.1}$$

where $\mathbf{n}$ and $\mathbf{n}'$ are unitary vectors along $\mathbf{k}$ and $\mathbf{k}'$, respectively. Using the definition of the propagation vector, $\mathbf{k} = (2\pi/\lambda)\,\mathbf{n}$ and $\mathbf{k}' = (2\pi/\lambda)\,\mathbf{n}'$, the interference condition can be written as

$$\frac{\lambda}{2\pi}\,\mathbf{R}(\mathbf{k}' - \mathbf{k}) = m\lambda \qquad \Rightarrow \qquad \mathbf{R}\,(\mathbf{k}' - \mathbf{k}) = 2\pi m \tag{5.2}$$

with integer m. This equation is known as the *Laue condition*. It should hold for every lattice vector $\mathbf{R}$ defined by Eq. (1.1), because a pair of atoms can be found for every such vector.

5.2. Reciprocal lattice

The vectors $\mathbf{k}' - \mathbf{k}$ satisfying the Laue condition form a *reciprocal lattice* of the crystal. One defines the reciprocal lattice as a family of vectors $\mathbf{G}$ that fulfill

$$e^{i\mathbf{G}\mathbf{R}} = 1 \tag{5.3}$$

for every lattice vector $\mathbf{R}$. It is common to say that $\mathbf{R}$'s belong to the direct lattice of the crystal in real space, whereas $\mathbf{G}$'s occur in the *reciprocal space*.

Reciprocal lattice can be constructed explicitly by choosing the vectors

$$\mathbf{a}^* = 2\pi\,\frac{[\mathbf{b}\times\mathbf{c}]}{\mathbf{a}\cdot[\mathbf{b}\times\mathbf{c}]}, \quad \mathbf{b}^* = 2\pi\,\frac{[\mathbf{c}\times\mathbf{a}]}{\mathbf{a}\cdot[\mathbf{b}\times\mathbf{c}]}, \quad \mathbf{c}^* = 2\pi\,\frac{[\mathbf{a}\times\mathbf{b}]}{\mathbf{a}\cdot[\mathbf{b}\times\mathbf{c}]}. \tag{5.4}$$

Then it is easy to verify that

$$\mathbf{a}^*\mathbf{a} = 2\pi, \quad \mathbf{a}^*\mathbf{b} = 0, \quad \mathbf{a}^*\mathbf{c} = 0 \tag{5.5}$$

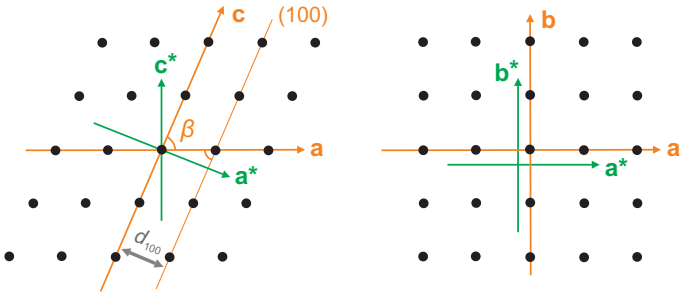

Figure 5.2: Direct-lattice and reciprocal-lattice vectors for the orthogonal (right) and non-orthogonal (left) lattice vectors. Note that the reciprocal-lattice vectors are not always parallel to those of the direct lattice, yet they are perpendicular to the corresponding lattice planes: for example, $\mathbf{a}^*$ is perpendicular to the (100) planes.

and so on, such that any vector

$$\mathbf{G} = h\mathbf{a}^* + k\mathbf{b}^* + l\mathbf{c}^* \tag{5.6}$$

with integer h, k, l satisfies the Laue condition, Eq. (5.2).

It is almost trivial to construct the reciprocal lattice when lattice vectors $\mathbf{a}, \mathbf{b}, \mathbf{c}$ are mutually orthogonal. In this case, $\mathbf{a} \cdot [\mathbf{b} \times \mathbf{c}] = abc$ and $[\mathbf{b} \times \mathbf{c}] \parallel \mathbf{a}$. Then $\mathbf{a}^* \parallel \mathbf{a}$ and $|\mathbf{a}^*| = 2\pi/a$, hence the name *reciprocal lattice*. Its directions are parallel to those of the direct lattice (Fig. 5.2), whereas reciprocal-lattice parameters are inverse of the lattice parameters in real space, times the pre-factor of 2π. This holds true for the orthorhombic, tetragonal, and cubic symmetries.

Other symmetries are more involved. Consider a monoclinic lattice with $\beta \neq 90°$. Then, $\mathbf{a} \cdot [\mathbf{b} \times \mathbf{c}] = abc \sin\beta$, and one finds

$$|\mathbf{a}^*| = \frac{2\pi}{a \sin\beta}, \quad |\mathbf{b}^*| = \frac{2\pi}{b}, \quad |\mathbf{c}^*| = \frac{2\pi}{c \sin\beta}. \tag{5.7}$$

Now, $\mathbf{a}^*$ and $\mathbf{c}^*$ are no longer parallel to $\mathbf{a}$ and $\mathbf{c}$ (Fig. 5.2). Instead, they form an angle of $\beta^* = 180° - \beta$.

We should also note that $\mathbf{a} \cdot [\mathbf{b} \times \mathbf{c}] = V$, the unit-cell volume in real space according to the standard definition of the triple product. To obtain unit-cell volume in the reciprocal space, one needs vector identities,

$$\mathbf{a}_1 \cdot [\mathbf{a}_2 \times \mathbf{a}_3] = \mathbf{a}_2 \cdot [\mathbf{a}_3 \times \mathbf{a}_1] \quad \text{and} \quad [\mathbf{a}_1 \times [\mathbf{a}_2 \times \mathbf{a}_3]] = \mathbf{a}_2(\mathbf{a}_3 \cdot \mathbf{a}_1) - \mathbf{a}_3(\mathbf{a}_1 \cdot \mathbf{a}_2), \tag{5.8}$$

that return

$$V^* = \mathbf{a}^* \cdot [\mathbf{b}^* \times \mathbf{c}^*] = \frac{2\pi}{V} [\mathbf{b} \times \mathbf{c}] \cdot [\mathbf{b}^* \times \mathbf{c}^*] = \frac{2\pi}{V} \mathbf{b}^* \cdot [\mathbf{c}^* \times [\mathbf{b} \times \mathbf{c}]] = \frac{(2\pi)^3}{V}. \tag{5.9}$$

This result will be needed in the future when we do summations over the reciprocal space.

At this point, reciprocal lattice may still look like a rather arbitrary mathematical construction, but it is in fact undeniably real because it is observed in every scattering experiment: intensity maxima appear at every or almost every (see Ch. 6.3) reciprocal-lattice site. We can also say that each crystal lives two parallel lives. One is in real space and constitutes tangible crystal properties. Another one is in the reciprocal space and incorporates intrinsic effects such as atomic vibrations and electronic transitions. Only by grasping reciprocal-space phenomena can one understand real-space properties of the crystal!

5.3. Relation to Bragg's law

The Laue condition and reciprocal lattice have a direct connection to Bragg's law. In fact, every reciprocal-lattice vector defined by Eq. (5.6) corresponds to the lattice planes with the Miller indices h, k, l. To verify this statement, choose the lattice planes (hkl) and define $\mathbf{n}$ as

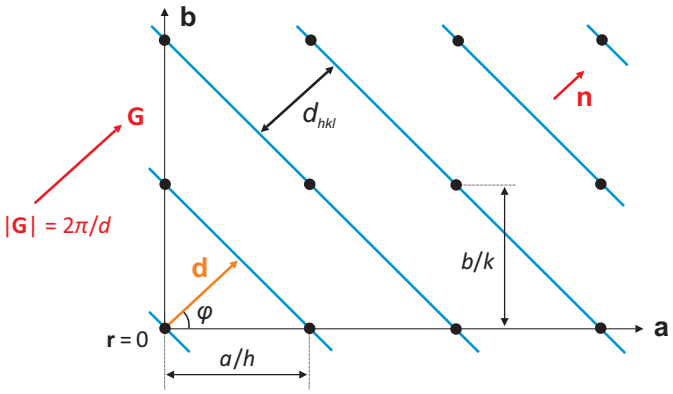

Figure 5.3: Relation between the reciprocal lattice and Bragg's law. The vector $\mathbf{G}$ chosen perpendicular to the lattice planes is a reciprocal-lattice vector. The Miller indices h, k, l define the representation of $\mathbf{G}$ in terms of $\mathbf{a}^*$, $\mathbf{b}^*$, $\mathbf{c}^*$.

the unitary vector perpendicular to these planes. Now choose $\mathbf{G} = 2\pi\mathbf{n}/d_{hkl}$ and consider it as a propagation vector of a wave with the wavelength of d_{hkl}. This wave has the form $e^{i\mathbf{Gr}}$. One expects $e^{i\mathbf{Gr}} = 1$ at $\mathbf{r} = 0$. Since $\mathbf{r} = 0$ corresponds to one of the lattice planes, the condition $e^{i\mathbf{Gr}} = 1$ should also hold on any other lattice plane because they are separated by an integer number of wavelengths (Fig. 5.3). Each point $\mathbf{R}$ of the direct lattice belongs to one or another lattice plane. Therefore, $e^{i\mathbf{GR}} = 1$ for every $\mathbf{R}$, and the condition (5.3) is fulfilled. Then $\mathbf{G}$ must be a reciprocal-lattice vector.

Now we have to prove that the reciprocal-lattice vector $\mathbf{G} = h\mathbf{a}^* + k\mathbf{b}^* + l\mathbf{c}^*$ corresponds to the planes with the Miller indices h, k, l. Let this vector define some lattice planes, which are perpendicular to it. We know that the corresponding interplane distance is given by $|\mathbf{G}| = 2\pi/d$. The distance between the origin and the nearest plane is a vector of the length d in the direction of $\mathbf{G}$ (Fig. 5.3), namely, $\mathbf{d} = d\,\mathbf{G}/|\mathbf{G}| = d^2\,\mathbf{G}/(2\pi)$. To determine the distance d_a that this plane intersects on the $\mathbf{a}$-axis, one has to compute

$$d_a = \frac{d}{\cos\varphi} = \frac{d}{\mathbf{d}\cdot\mathbf{a}/(da)} = \frac{2\pi a}{\mathbf{G}\cdot\mathbf{a}} = \frac{2\pi a}{h\,\mathbf{a}^*\cdot\mathbf{a}} = \frac{a}{h}, \tag{5.10}$$

which is equivalent to Eq. (4.3) that served as the definition of the Miller indices h, k, l.

We now realize that the lattice planes used in Bragg's law are real-space manifestations of the reciprocal lattice. Incident light sees crystal as an optical grating, with different gratings identified by different families of the lattice planes. There need not be atoms on a given lattice plane to produce a Bragg peak. The positions of these Bragg peaks define the reciprocal lattice and directly convey lattice parameters of the crystal.

This statement also sheds light on Eq. (4.4) for d_{hkl} that immediately follows from $|\mathbf{G}|^2 = h^2|\mathbf{a}^*|^2 + k^2|\mathbf{b}^*|^2 + l^2|\mathbf{c}^*|^2$ as the vector length in the reciprocal space (assuming $\mathbf{a}, \mathbf{b}, \mathbf{c}$ are mutually orthogonal). The calculation of d_{hkl} for an arbitrary lattice also becomes straightforward, albeit tedious when non-90° angles have to be taken into account.

5.4. Aperiodic crystals

We can also see reciprocal lattice as a Fourier transform of the direct lattice. Bragg peaks at the reciprocal-lattice points indicate periodicity of the crystal in real space. This statement is in fact much more general, because aperiodic crystals also show characteristic diffraction patterns with a series of Bragg peaks. Such peaks manifest the underlying long-range order of the aperiodic crystal. The difference from periodic crystals is that the reciprocal lattice spun by $\mathbf{a}^*$, $\mathbf{b}^*$, and $\mathbf{c}^*$ is no longer sufficient to describe the Bragg peaks.

Many of the aperiodic crystals can be seen as *modulated structures*. Their diffraction patterns are described by a 3D reciprocal lattice plus one or more additional vectors $\mathbf{t}_i$ known as modulation vectors. Mathematically, these $\mathbf{t}_i$'s can be still decomposed into reciprocal-lattice

vectors,

$$\mathbf{t}_i = p_1\mathbf{a}^* + p_2\mathbf{b}^* + p_3\mathbf{c}^*. \tag{5.11}$$

When p_1, p_2, p_3 are simple fractions like $\frac{1}{2}$ or $\frac{1}{5}$, the structure is called *commensurately modulated*. It is nothing but a periodic crystal with the larger unit cell. For example, $p_1 = \frac{1}{2}$ would mean that $\mathbf{a}^*$ should be twice shorter, hence the lattice parameter a should be twice longer: some element of the structure develops a twice longer periodicity than the rest of the crystal and requires a two-fold expansion of the unit cell. By contrast, a structure with random values of p_1, p_2, p_3 is *incommensurately modulated*.

Special mathematical formalism has been developed for modulated structures. It is based on a proper (periodic) lattice defined in a $3 + n$-dimensional space known as *superspace* where modulation vectors $\mathbf{t}_i$ are accommodated along additional, artificial dimensions, in order to restore periodicity of the system. For example, quasicrystals can be described as periodic structures in the 5D or 6D reciprocal space. This space is, of course, unphysical, but its 3D projection forms the physical reciprocal space where diffraction pattern is observed. The introduction of additional dimensions may seem bizarre at first glance, but it becomes more palatable if one considers that crystallographic restriction theorem forbids 5-fold symmetry only in 3D space. In higher dimensions, five-fold rotations may be compatible with periodicity.

Incommensurate modulations may have different origin depending on the chemical nature of the crystal. Sometimes it is related to deformations or rotations of structural units that occupy a certain position in space, but vary with a different periodicity compared to the rest of the lattice. Other examples of aperiodic crystals are framework structures with channels where atoms in channels have their own periodicity compared to the framework. Aperiodic crystals are inconspicuous but abundant. They may occur in elemental solids, including Bi and Te under pressure, or in such a common material as Na_2CO_3, better known as washing soda. A short memorial article can serve as a good introduction into aperiodic crystals.

6. Structure factor: All shades of diffraction

6.1. Structure factor

Reciprocal lattice serves as a connection between positions of Bragg peaks and lattice parameters of the crystal. Similarly, structure factor connects intensities of Bragg peaks to the atomic coordinates.

To calculate intensity of a Bragg peak, we go back to Laue's representation of the scattering process and take the scattering mechanism into account. Atoms are not point-like objects, and atoms are not scatterers *per se*. Instead, one should consider periodic scattering density $\rho(\mathbf{r})$ that satisfies $\rho(\mathbf{r}+\mathbf{R}) = \rho(\mathbf{r})$ for every lattice vector $\mathbf{R}$.

Every small volume element $\mathbf{dr}$ scatters the incident wave. The phase of the scattered wave depends on the position of $\mathbf{dr}$ inside the crystal. Indeed, from Laue's argument (Ch. 5.1) the path difference for a given position $\mathbf{r}$ relative to the origin is

$$\frac{\lambda}{2\pi}\,\mathbf{r}(\mathbf{k}-\mathbf{k}') = \frac{\lambda}{2\pi}\,\mathbf{G}\,\mathbf{r} \tag{6.1}$$

and the corresponding phase shift is $\Delta\varphi = \mathbf{G}\,\mathbf{r}$ where $\mathbf{G}$ is a reciprocal-lattice vector. The scattered wave is obtained by integrating such phase shifts over the unit cell, taking into account $\rho(\mathbf{r})$ as the concentration of scatterers in a given position $\mathbf{r}$,

$$e^{i(\mathbf{k}'\tilde{\mathbf{r}}-\omega t)} \cdot \int \rho(\mathbf{r})\, e^{i\mathbf{G}\mathbf{r}}\,\mathbf{dr} = e^{i(\mathbf{k}'\tilde{\mathbf{r}}-\omega t)}\, F(\mathbf{G}) \tag{6.2}$$

where the newly introduced *structure factor* $F(\mathbf{G})$ is the amplitude of the scattered wave that travels away from the crystal into some arbitrary position $\tilde{\mathbf{r}}$. Intensity is proportional[8] to the squared amplitude,

$$I(\mathbf{G}) \sim |F(\mathbf{G})|^2, \qquad F(\mathbf{G}) = \int\limits_{\mathrm{UC}} \rho(\mathbf{r})\, e^{i\mathbf{G}\mathbf{r}}\,\mathbf{dr}. \tag{6.3}$$

Considering the periodicity of $\rho(\mathbf{r})$, it is sufficient to integrate over the unit cell (UC) when calculating $F(\mathbf{G})$, because other unit cells will simply lead to an additional pre-factor, which should be the same for every reflection.[9]

It is instructive to compare the structure factor, Eq. (6.3), with the Fourier decomposition of the scattering density,

$$\rho(\mathbf{r}) = \sum_{\mathbf{G}} \rho_{\mathbf{G}}\, e^{i\mathbf{G}\mathbf{r}}, \qquad \rho_{\mathbf{G}} = \frac{1}{V}\int \rho(\mathbf{r})\, e^{i\mathbf{G}\mathbf{r}}\,\mathbf{dr}, \tag{6.4}$$

where we restricted the summation to the reciprocal-lattice vectors $\mathbf{G}$ because $\rho(\mathbf{r})$ is periodic in direct space. In fact, structure factor is merely the Fourier component of the scattering density, up to a pre-factor.

6.2. Atomic approximation

Strictly speaking, it is not necessary to think of atoms when we calculate $F(\mathbf{G})$, but life becomes easier when we do, namely, when the scattering density $\rho(\mathbf{r})$ is represented as a superposition

[8] Experimentally, intensity depends on the exposure time and can be defined up to a scale factor, only.

[9] An adverse consequence of this multiplication is that $F(\mathbf{G})$ and $I(\mathbf{G})$ go to infinity in thermodynamic limit (for an infinite crystal). This is the drawback of the kinematic theory that neglects multiple scattering, although, as a matter of fact, a scattered wave should scatter again, and again, and again when the crystal is infinite. Such a multiple scattering is taken into account in the dynamic theory of diffraction that we will not consider here because for many practical purposes the kinematic theory suffices.

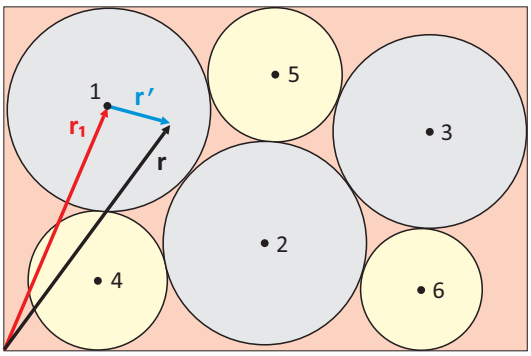

Figure 6.1: Scattering density of the crystal, $\rho(\mathbf{r})$, is represented as a superposition of the scattering densities of individual atoms, $\rho_j(\mathbf{r}')$, with the vector $\mathbf{r}$ decomposed into $\mathbf{r}_1 + \mathbf{r}'$.

of scattering densities $\rho_j(\mathbf{r}')$ from individual atoms. Consider $j = 1, \dots N$ atoms located at the positions $\mathbf{r}_1, \dots \mathbf{r}_N$ within the unit cell. By introducing the volume element $\mathbf{dr}'$ within an atom, we represent $\mathbf{r} = \mathbf{r}_j + \mathbf{r}'$ (Fig. 6.1) and re-write the structure factor as a sum over individual atoms,

$$F(\mathbf{G}) = \int \rho(\mathbf{r})\, e^{i\mathbf{G}\mathbf{r}}\, \mathbf{dr} = \sum_{j=1}^{N} e^{i\mathbf{G}\mathbf{r}_j} \int\limits_{\text{atom}} \rho_j(\mathbf{r}')\, e^{i\mathbf{G}\mathbf{r}'} \mathbf{dr}' = \sum_{j=1}^{N} f_j(\mathbf{G})\, e^{i\mathbf{G}\mathbf{r}_j}. \tag{6.5}$$

Here, we introduced the *atomic form factor* $f_j(\mathbf{G})$ that describes the scattering of the wave by a given atom j in the direction of $\mathbf{G}$.

To a first approximation, any given atom scatters waves in the same way regardless of the chemical environment of this atom. Then the same set of atomic form factors can be used for all crystals, and the variation of the Bragg peak intensity with $\mathbf{G}$ arises from two ingredients:

- *material-specific:* positions of atoms $\mathbf{r}_j$ within the unit cell
- *generic:* angular dependence of the scattering by a given atom, as defined by $f_j(\mathbf{G})$, regardless of the exact nature of the crystal

6.3. Extinction conditions

The structure factor defined by Eq. (6.3) reflects the arrangement of atoms inside the crystal. Experimental structure factors can be used to determine atomic positions, as we will further discuss in Ch. 6.4. Interestingly, using only a simple maths one can draw some conclusions on the symmetry of the crystal when lattice centering (Ch. 2.2) or open symmetry elements (Ch. 3.4) connect different atoms therein.

i) Lattice centering. Consider a body-centered crystal structure with the lattice translation of $\mathbf{t} = \frac{1}{2}(\mathbf{a}+\mathbf{b}+\mathbf{c})$. Then an atom located at (x, y, z) has a counterpart at $(x+\frac{1}{2}, y+\frac{1}{2}, z+\frac{1}{2})$. Using the standard representation $\mathbf{G} = h\mathbf{a}^* + k\mathbf{b}^* + l\mathbf{c}^*$, one finds

$$\mathbf{G}\,\mathbf{r}_j = (h\mathbf{a}^* + k\mathbf{b}^* + l\mathbf{c}^*)(x_j\mathbf{a} + y_j\mathbf{b} + z_j\mathbf{c}) = 2\pi(hx_j + ky_j + lz_j) \tag{6.6}$$

(note an immediate advantage of fractional atomic coordinates in conjunction with the reciprocal lattice!) We can now write the structure factor as

$$\begin{aligned} F(\mathbf{G}) = \sum_{j=1}^{N} f_j(\mathbf{G})\, e^{i\mathbf{G}\mathbf{r}_j} &= \sum_{j=1}^{N/2} f_j(\mathbf{G}) \left[e^{2\pi i(hx_j+ky_j+lz_j)} + e^{2\pi i\left[h(x_j+\frac{1}{2})+k(y_j+\frac{1}{2})+l(z_j+\frac{1}{2})\right]} \right] \\ &= \sum_{j=1}^{N/2} f_j(\mathbf{G})\, e^{2\pi i(hx_j+ky_j+lz_j)} \left[1 + e^{\pi i(h+k+l)}\right] \end{aligned} \tag{6.7}$$

The expression in square brackets can be either 0 or 2 depending on whether $h+k+l$ is odd or even, respectively. We thus see that lattice centering defines a special rule for the reflection

intensities. Only reflections with $h + k + l = 2n$ (even) are observed. This is the *reflection condition* for a body-centered crystal. The systematic absence of reflections is known as an *extinction*, so we could also introduce an extinction condition $h + k + l = 2n + 1$ (odd).

ii) Open symmetry elements. Glide planes and screw axes cause their own extinctions. Consider the glide plane $a \perp \mathbf{c}$. It leads to the transformation $(x, y, z) \to (x + \frac{1}{2}, y, \bar{z})$. Then the structure factor becomes

$$F(\mathbf{G}) = \sum_{j=1}^{N/2} f_j(\mathbf{G}) \left[e^{2\pi i(hx_j + ky_j + lz_j)} + e^{2\pi i\left[h(x_j + \frac{1}{2}) + ky_j - lz_j\right]} \right]. \tag{6.8}$$

This expression does not look very spectacular, but it becomes simpler in the special case of $l = 0$. Then,

$$F_{hk0} = \sum_{j=1}^{N/2} f_j(hk0)\, e^{2\pi i(hx_j + ky_j)} \left[1 + e^{\pi i h}\right] \tag{6.9}$$

and we expect the reflection condition $hk0, h = 2n$ for the a-glide plane perpendicular to $\mathbf{c}$.

Reflection conditions for a given space group can be obtained from the HKLCOND utility at the Bilbao Server. By analyzing extinctions, crystal symmetry can be determined or, more precisely, narrowed down to a list of possible space groups.

More generally, one can see the reflection (extinction) conditions as a manifestation of the periodicity. The reciprocal lattice defined using three lattice vectors, Eq. (5.4), corresponds to the situation when no additional translations are allowed. Crystals with lattice centering have a shorter periodicity indicated by the primitive cell, so their reciprocal lattices should be more sparse. This effect is achieved by removing some of the reciprocal-lattice points via extinctions. For example, reciprocal lattice of a bcc lattice is an fcc lattice with the periodicity of $4\pi/a$.

6.4. Crystal structure determination

Crystal structures are determined from diffraction experiments that involve an accurate measurement of both position and intensity for every Bragg peak. The structure solution includes three consecutive steps:

- *indexing* of the Bragg peaks, finding lattice parameters from the peak positions
- *analyzing* extinctions in order to determine the crystal symmetry[10]
- *finding* a structural model that gives the best fit to the experimental Bragg peak intensities

The principal advantage of the diffraction methods is that many Bragg peaks can be measured in order to determine atomic positions with a very high accuracy. A typical diffraction experiment covers thousands of Bragg peaks, and interatomic distances are determined with an uncertainty of less than 0.01 Å. Such a high spatial resolution is only possible with the reciprocal-space technique (measurement of Bragg peaks in the reciprocal space) and can not be matched by the direct-space imaging with electron microscopy (Ch. 1.3).

6.5. Atomic form factors

From Eq. (6.5), atomic form factor is defined as the Fourier-transformed scattering density $\rho(\mathbf{r})$ of a single atom,

$$f(\mathbf{q}) = \int \rho(\mathbf{r})\, e^{i\mathbf{qr}}\, \mathbf{dr} \tag{6.10}$$

[10] More precisely, lattice centering can be determined, and a subset of possible space groups defined. Space groups that contain neither lattice centering nor open symmetry elements do not have any reflection conditions and can not be distinguished in this way.

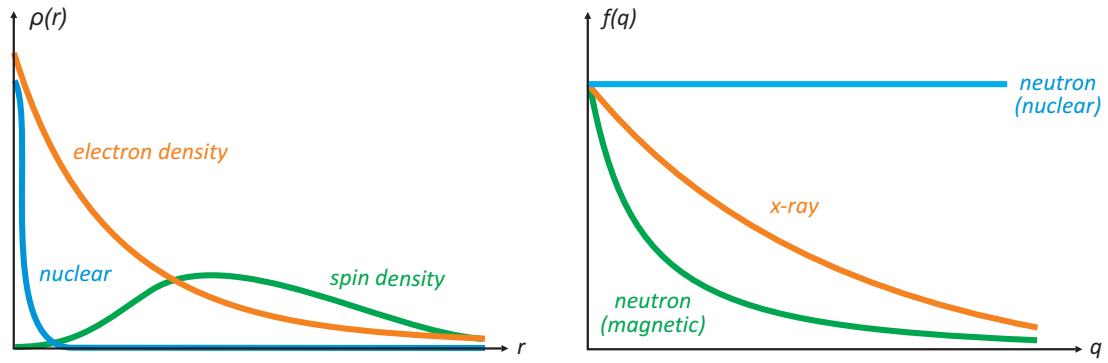

Figure 6.2: Scattering densities (left) and the resulting atomic form factors (right) for the x-ray and neutron scattering. Different densities are not drawn to the scale. Spin density is typically associated with the d- and f-atomic orbitals that have nodes at $r = 0$.

where $\mathbf{q}$ is a vector in the reciprocal space (the vectors $\mathbf{q}$ are no longer restricted to the reciprocal-lattice vectors $\mathbf{G}$, because atom is not periodic). Spherical symmetry of an atom implies that f depends only on $|\mathbf{q}|$ and not on the direction of $\mathbf{q}$. It is then customary to represent $|\mathbf{q}|$ as $2\pi/d$ similar to Ch. 5.3 and consider $1/d \sim \sin\theta/\lambda$ from Bragg's law. Therefore, atomic form factors are tabulated as a function of $\sin\theta/\lambda$, measured in Å^{-1}. They can be found in the International Tables for Crystallography and on the web.

The scattering density in Eq. (6.10) depends on the nature of the wave being scattered. Several cases are of special importance (Fig. 6.2):

- *x-rays* are scattered by electrons, so $\rho(\mathbf{r})$ is electron density that gradually decreases away from the atom. Then $f(\mathbf{q})$ is also a slowly decreasing function. Larger values of $|\mathbf{q}|$ correspond to smaller values of d_{hkl} that, in turn, correspond to the higher angles θ. Therefore, one sees lower intensities in XRD patterns at high angles
- *neutrons* are scattered by the atomic nuclei, which are very small. Then, $\rho(\mathbf{r})$ looks more like a δ-function, while its Fourier transform is a constant. In a neutron diffraction experiment, reflection intensities only weakly depend on the angle θ.
- *neutrons* are also scattered by the spin density, namely, by valence electrons with an unpaired spin. This is the primary experimental tool for studying magnetic order in crystals. The corresponding magnetic form factor decreases even faster than the x-ray one because only valence electrons are involved, so magnetic Bragg peaks are observed at low angles only
- *electrons* are scattered by other electrons, so their $f(\mathbf{q})$ is similar to that of x-rays. The intensities decrease with the angle. However, electrons are impatient and will usually scatter several times as they travel through the crystal. Intensities of Bragg peaks in electron diffraction are, therefore, strongly affected by multiple scattering.

6.6. Neutron diffraction

Neutrons can be an alternative to x-rays in the diffaction experiments. The main advantage of neutrons is their sensitivity to light elements. Since x-rays are scattered by electrons, the x-ray atomic form factor scales with the number of electrons, i.e., the atomic number Z. Then the quadratic scaling of the reflection intensity, $I \sim Z^2$, leads to a very sharp difference between the scattering from heavy and light elements. Ultimately, hydrogen atoms scatter so weakly that they become hard to locate using x-rays.

Neutrons are scattered by the atomic nuclei with no systematic dependence on Z, so they can be used to locate light elements in the crystal structure. Another advantage is the sensitivity

of neutrons to magnetic order, the feature that x-rays lack.[11]

Neutron diffraction experiments have major downsides too. Neutrons can not be produced in the lab, they are obtained either from a nuclear reactor or from a so-called spallation source. Both are huge installations, and only a handful of neutron research facilities exist around the world. Neutron beams are hard to focus, so large instrumentation is needed, and sample volume is usually much larger than in the case of x-rays. Tiny objects like thin films are hard to study using neutrons, and spatial resolution is much lower.

[11] Unless experiments are performed at the x-ray energy that matches the absorption edge, see resonant x-ray scattering.

7. Bonding in crystals: ionic

7.1. Types of chemical bonding

Many of the crystal properties can be understood from the perspective of bonding between the atoms. Four main types of chemical bonding are usually distinguished:

- *ionic*, due to electrostatic forces between charged units (ions)
- *covalent*, due to an overlap of atomic orbitals
- *metallic*, due to shared (itinerant) electrons
- *van der Waals*, due to dipole-dipole and other weak interactions, such as London dispersion force (between induced dipoles)

One often identifies a separate group of *hydrogen bonds*, which occur between atoms with small, fractional charges, such as H and O in water and organic molecules. These bonds are somewhat stronger than the typical van der Waals bonds, yet for our purpose they fall into the same group of weak bonding. We will also discuss *molecular crystals* where finite units (molecules) formed by covalent bonds are held together by van der Waals bonds.

7.2. Cohesive and lattice energies

Stability of the crystal is characterized by its energy. In this context, two closely related energies can be defined. *Cohesive energy* is the energy required to break the crystal into individual atoms. *Lattice energy* is the energy required to split the crystal into its constituents.[12] The cohesive and lattice energies are equal for metallic crystals and for simple covalent crystals like diamond. However, they are very different in molecular crystals where molecules formed by covalent bonds are held together by van der Waals bonds. In this case, only lattice energy is the relevant energy scale because it shows the energy cost of breaking the crystal into individual molecules (think of sublimation of iodine into a gas of I_2 molecules). A somewhat similar situation occurs in ionic crystals. Compare

$$\begin{aligned} \mathrm{AB}_{(s)} + \mathcal{E}_{\mathrm{coh}} &\longrightarrow \mathrm{A}_{(g)} + \mathrm{B}_{(g)}, \\ \mathrm{AB}_{(s)} + \mathcal{E}_{\mathrm{lat}} &\longrightarrow \mathrm{A}^{+}_{(g)} + \mathrm{B}^{-}_{(g)} \end{aligned}$$

where the subscripts (s) and (g) denote the solid and gas states, respectively.

Lattice energies are obtained from *calorimetry experiments* where the amount of heat released or absorbed in a given process is measured. Sublimation enthalpy of a metallic, covalent, or molecular crystal is a direct measure of its lattice energy.[13] More often, though, the quantity measured in the experiment is the formation enthalpy $\Delta_f H$, which is neither cohesive nor lattice energy of the crystal:

$$\mathrm{Na}_{(s)} + \tfrac{1}{2}\mathrm{Cl}_{2\,(g)} \longrightarrow \mathrm{NaCl}_{(s)} + \Delta_f H$$

This formation enthalpy can be related to the lattice energy by considering all intermediate processes (Fig. **??**) and adding up relevant energies: sublimation energy of the Na metal, ionization potential of the Na atom, bond dissociation energy of the Cl_2 molecule, and electron

[12] Older textbooks, including the one by Ashcroft and Mermin define cohesion energy simply as lattice energy and describe the formation of crystal from its constituents as *cohesion*.

[13] In thermochemistry, enthalpies are commonly used instead of energies because measurements are performed at a constant pressure rather than constant volume. Then, strictly speaking, lattice *enthalpy* is obtained. This difference is usually unimportant, since solids show only a minor difference between energy and enthalpy owing to the small thermal expansion, see also Ch. **??**.

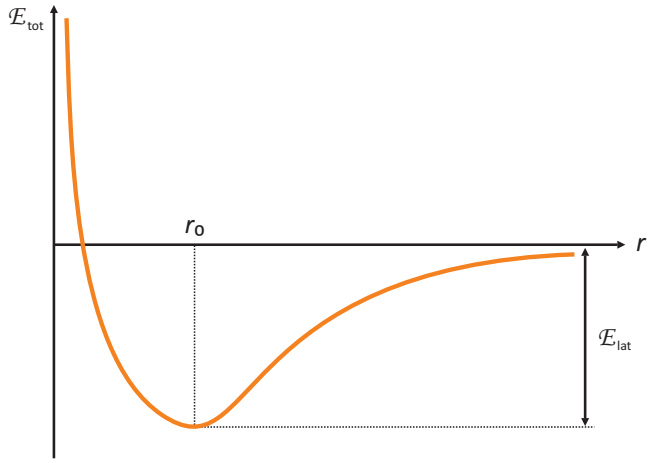

Figure 7.1: Crystal energy $\mathcal{E}_{\text{tot}}$ as a function of the interatomic distance r. Lattice parameters define the equilibrium value r_0, while the depth of the energy minimum is the lattice energy $\mathcal{E}_{\text{lat}}$.

affinity of the Cl atom. All these quantities can be measured in separate experiments, and eventually lattice energy of NaCl can be obtained from $\Delta_f H$ of NaCl. This method is known as the *Born-Haber cycle*. Thermochemistry data can be found in multiple sources, such as NIST Chemistry WebBook and CRC Handbook of Chemistry and Physics.

It is also helpful to represent crystal energy as a function of an effective interatomic distance, $\mathcal{E}(r)$, as shown in Fig. 7.1. Then the position of the energy minimum yields the equilibrium distance r_0 and, consequently, the lattice parameter of the crystal. The depth of the minimum is the lattice energy $\mathcal{E}_{\text{lat}}$.

7.3. Madelung constant

We will now concentrate on the ionic crystals and try to calculate $\mathcal{E}(r)$. To this end, we assume that the interatomic forces are Coulomb in nature and determine the electrostatic potential at a given site i,

$$\mathcal{V}_i = \frac{e}{4\pi\varepsilon_0} \sum_j \frac{z_j}{r_{ij}} \tag{7.1}$$

where z_j is the ionic charge and r_{ij} is the distance between ions. This summation can be replaced with

$$\mathcal{V}_i = \frac{e}{4\pi\varepsilon_0} \frac{\alpha_i}{r} \tag{7.2}$$

where r stands for the nearest-neighbor distance and α_i is the *Madelung constant* for the site i. This Madelung constant is defined for a given structure type and ionic charge and does not depend on the exact lattice parameter. Getting the actual values of α_i is far from trivial because Coulomb interactions are long-range, and the series defined by Eq. (7.1) is conditionally convergent.[14] One practical approach to this problem is the Ewald summation.

Coulomb energy of the crystal can be then written as

$$\mathcal{E}_{\text{Coul}} = \tfrac{1}{2} \sum_i e z_i \mathcal{V}_i = \tfrac{1}{2} \sum_i \frac{e^2 z_i \alpha_i}{4\pi\varepsilon_0 r} \tag{7.3}$$

with the pre-factor $\frac{1}{2}$ to avoid double-counting. This summation will include several terms according to the number of different atomic positions in the crystal. In a simple AB crystal, symmetry requires that $\alpha_+ = \alpha_- = \alpha$. Using $z_+ = -z_- = z$, one finds

$$\mathcal{E}_{\text{Coul}} = -\frac{\alpha z^2 e^2}{4\pi\varepsilon_0 r} \tag{7.4}$$

[14] Some instructive examples of the conditional convergence of electrostatic energy in ionic crystals can be found here and here.

This energy does not have a minimum, and indeed an ionic crystal with only Coulomb forces should collapse. An energy minimum in the vein of Fig. 7.1 appears when Coulomb energy is augmented by a repulsive energy,

$$\mathcal{E}_{\text{tot}}(r) = -\frac{\alpha z^2 e^2}{4\pi\varepsilon_0 r} + \frac{C_{\text{rep}}}{r^m} \tag{7.5}$$

where $C_{\text{rep}} = \text{const}$ and m is also a constant that takes values between 6 and 10 depending on the ions. This repulsive potential is empirical in nature and mimics the intuitive understanding that different atoms cannot penetrate into each other. Beyond this common intuition, the repulsion goes back to the Pauli exclusion principle, as explained here.

7.4. Born-Landé equation

Equilibrium distance r_0 corresponds to the energy minimum of $\mathcal{E}_{\text{tot}}(r)$ from Eq. (7.5),

$$\frac{d\mathcal{E}_{\text{tot}}}{dr} = 0 \;\Rightarrow\; \frac{\alpha z^2 e^2}{4\pi\varepsilon_0 r_0^2} - m\frac{C_{\text{rep}}}{r_0^{m+1}} = 0 \;\Rightarrow\; r_0^{m-1} = 4\pi\varepsilon_0 \frac{mC_{\text{rep}}}{\alpha z^2 e^2} \;\Rightarrow\; C_{\text{rep}} = \frac{\alpha z^2 e^2}{4\pi\varepsilon_0 m} r_0^{m-1} \tag{7.6}$$

It can be used to calculate lattice energy,

$$\mathcal{E}_{\text{lat}} = -\mathcal{E}_{\text{tot}}(r_0) = \frac{\alpha z^2 e^2}{4\pi\varepsilon_0 r_0} - \frac{\alpha z^2 e^2}{4\pi\varepsilon_0 r_0}\frac{1}{m} = \frac{\alpha z^2 e^2}{4\pi\varepsilon_0 r_0}\left(1 - \frac{1}{m}\right), \tag{7.7}$$

resulting in the *Born-Landé equation* for ionic crystals.

This equation has some immediate implications:

- lattice energy of an ionic crystal increases with the ionic charge; therefore, oxides ($z = 2$) usually have much higher melting points than halides ($z = 1$)
- lattice energy of an ionic crystal decreases with the interatomic distance (r_0); therefore, melting points decrease from NaF to NaI and from NaF to CsF and correlate with the lattice parameter

Typical lattice energies of ionic crystals are in the range of $5 - 10\,\text{eV/f.u.}$ Born-Landé equation can also be used to calculate lattice energy for the known interatomic distance, which is usually determined by XRD. The unknown parameter m enters the energy as $1/m$ and changes the result only marginally. This parameter can be determined when another experimental observable, such as bulk modulus, is available.

7.5. Bulk modulus

The isothermal *bulk modulus* is defined as

$$B = -V\left(\frac{\partial p}{\partial V}\right)_T \tag{7.8}$$

It shows the change in the crystal volume under pressure (more on this in Ch. 9.1). The bulk modulus can be obtained from $\mathcal{E}_{\text{tot}}$ if one considers thermodynamic definition of pressure, $p = -(\partial\mathcal{E}/\partial V)_T$. The bulk modulus is essentially the second derivative of $\mathcal{E}_{\text{tot}}$ with respect to V. In contrast to lattice energy, Eq. (7.7), the exact expression for the bulk modulus depends on the structure type, which defines the relation between V and r in the crystal.

Let's choose rocksalt-type structure (Ch. 7.6) as an example. The distance r is the separation between the cation and anion, $r = a/2$. Then, $V = a^3/4 = 2r^3$ (volume per formula unit) and

$$\frac{d}{dV} = \frac{1}{6r^2}\frac{d}{dr} \;\Rightarrow\; B = V\frac{d}{dV}\frac{d\mathcal{E}_{\text{tot}}}{dV} = \frac{r}{18}\frac{d}{dr}\left(\frac{1}{r^2}\frac{d\mathcal{E}_{\text{tot}}}{dr}\right). \tag{7.9}$$

This value should be taken at $r = r_0$ where $d\mathcal{E}_{\text{tot}}/dr = 0$. Then, the equation simplifies to

$$B = \frac{1}{18\, r_0} \left. \frac{d^2\mathcal{E}_{\text{tot}}}{dr^2} \right|_{r=r_0} = \frac{m-1}{18} \frac{\alpha z^2 e^2}{4\pi\varepsilon_0 r_0^4} \tag{7.10}$$

where we used Eq. (7.6) to express C_{rep} via r_0.

Clearly, bulk modulus shows the same trends as lattice energy. Oxides are less compressible than halides, that is, they feature higher bulk moduli. Compressibility of an ionic crystal increases upon increasing its lattice parameter. By measuring both B and r_0, the value of m and, eventually, the exact lattice energy can be determined. Typical bulk moduli of ionic crystals are in the range of $10 - 200$ GPa.

7.6. Ionic radius and Pauling's rule

Whereas the Born-Landé equation, Eq. (7.7), offers a simple explanation for changes in lattice energy, melting points, and bulk moduli across different ionic crystals, it fails to answer one fundamental question: which structure type is chosen by a given ionic material? The Madelung constants for different structure types can be compared, but how to deal with the distance r_0?

Typical values of r_0 can be obtained from the so-called *ionic radii* that have been estimated for every possible ion of every chemical element by analyzing the statistics of interatomic distances in thousands of crystal structures determined experimentally. One assumes $r_0 \simeq r_+ + r_-$ and finds the optimal values of r_+ and r_- that fit the experimental r_0 in different materials. Different sets of ionic radii exist, the most common one being the system by Shannon and Prewitt quoted in multiple handbooks, for example here. Because the ionic radii are determined from the experimental data, they take different values depending not only on the ionic charge but also on the coordination number. Increasing the charge and/or the coordination number reduces ionic radius of a cation. The opposite is true for anions, which are generally larger than cations because adding an electron requires extra space.

Ionic radii are often sufficient to analyze structure types of different ionic crystals. *Pauling's first rule*[15] postulates that the coordination number of a cation in an ionic crystal is determined by the ratio r_+/r_-. This rule goes back to a simple geometrical argument that anions should not come too close to each other. Therefore, smaller cations require lower coordination numbers. The threshold values of r_+/r_- have been derived as follows:

CN	*polyhedron*	r_+/r_- *larger than*
3	triangle	0.155
4	tetrahedron	0.225
6	octahedron	0.414
8	cube	0.732

The most common coordination numbers are 4 and 6. Representative structure types are *zinc blende* and *rocksalt* shown in Fig. 7.2. Very large cations like Cs^+ may form *CsCl-type* structures with the cubic coordination.

Pauling's consideration of the ionic radii inspires polyhedral description of ionic crystals. Anions form the polyhedron around a cation. By defining these polyhedra, the connectivity of the structure can be analyzed.

[15] Four other Pauling's rules are even more empirical and can be found here.

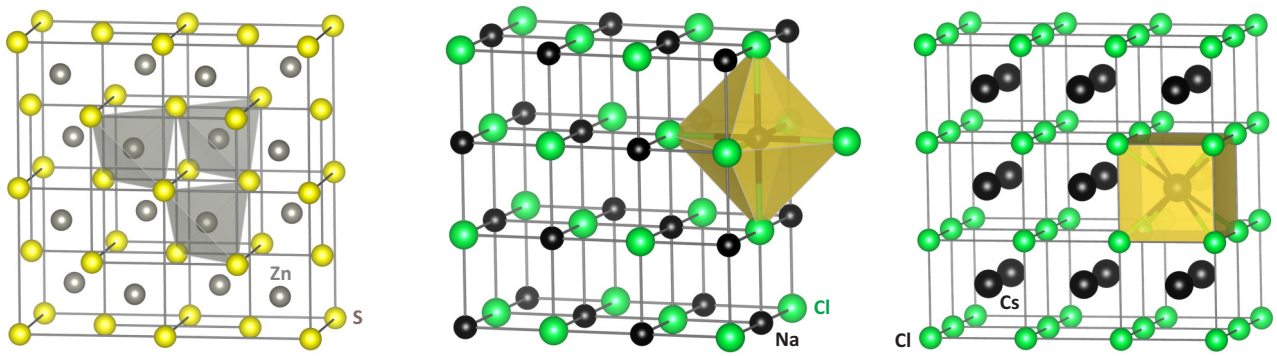

Figure 7.2: Common structure types of ionic crystals: zinc blende (fcc lattice), rocksalt (fcc lattice), and CsCl-type (primitive cubic lattice).

7.7. Ionic crystals as close-packed structures

Structures of ionic crystals can be also analyzed from the perspective of close packing. Anions form close-packed layers because they are usually bigger than cations. Then cations fill octahedral and tetrahedral voids between these close-packed layers. There is one octahedral and two tetrahedral voids per anion.

Let anions form the cubic close packing:

- filling octahedral voids yields the rocksalt structure (NaCl)
- filling $\frac{1}{2}$ of the tetrahedral voids yields the zinc blende structure (ZnS, CdTe)
- filling all tetrahedral voids yields the fluorite structure (CaF_2). Note that in fluorite cations form the close-packed structure, whereas anions occupy the tetrahedral voids. The situation is reversed in antifluorite (Na_2O) where anions form the close-packed structure and anions are in the voids.
- filling octahedral and $\frac{1}{2}$ of the tetrahedral voids yields the spinel structure ($MgAl_2O_4$)

A similar construction is possible for the hexagonal close packing of anions too:

- filling octahedral voids yields the NiAs structure (MnS)
- filling $\frac{1}{2}$ of the tetrahedral voids yields the wurtzite structure (ZnS, AgI)

This simple principle describes many of the common structure types of ionic compounds and also elucidates their hexagonal or fcc symmetries. However, it is not always easy to understand which structure type is preferred by a given compound. One compound may form different structures as in the case of ZnS. This is an example of *polymorphism*.

8. Bonding in crystals: covalent, metallic, and van der Waals

8.1. Covalent crystals

The formation of covalent bonds can be probed using the *covalent radius*.[16] When $r_{AB} \leq r_A + r_B$, a covalent bond occurs between the atoms A and B. Shorter distances indicate stronger covalent bonds. This is well known from carbon in organic molecules where single (1.54 Å), double (1.34 Å), and triple (1.20 Å) C–C bonds can be distinguished by their typical length and chemical environment. Covalent bonds in solids are not always identifiable as single, double, or triple, but the same trend holds.

Complex nature of the covalent bonds does not allow a generic description in the same vein as Eq. (7.5). We can only say that shorter covalent bonds should lead to the increased lattice energy and higher bulk modulus. The typical lattice energies of covalent crystals are on the order of 10 eV/atom and the bulk moduli are in the range of $50 - 200$ GPa.

8.2. Metallic crystals

There is not much to say about metallic crystals at this stage. We will address them in more detail in Ch. **??**. For now let's mention without any explicit derivation that lattice energy of a metallic crystal is given by a rather non-intuitive expression

$$\mathcal{E}_{\text{lat}} = \frac{3\,\hbar^2}{10\,m_e}(3\pi^2 n_e)^{\frac{2}{3}}, \tag{8.1}$$

so it depends on the electron concentration n_e and decreases with increasing the lattice parameter.

Metals can have lattice energies as low as 1 eV/atom and feature bulk moduli of several GPa only. Some of the elemental metals have melting points close to room temperature (cesium, gallium), whereas mercury is even a liquid. Nevertheless, other metals like tungsten are characterized by very high melting points and low compressibilities, exceeding those of the typical ionic crystals. It all depends on the electron concentration.

8.3. Polymorphism

In elemental solids, the type of the crystal structure will be usually determined by chemical bonding. Metals tend to adopt simple and dense structures (see Ch. 1.2), non-metals will often develop similar structures but with the packing of weakly bonded atoms (noble gases) or diatomic molecules (hydrogen, oxygen). Elements spanning the boundary between metals and non-metals show the most diverse behavior, as they can form different types of covalently-bonded structures and simultaneously appear in the metallic form. Tin is a celebrated example. It forms metallic crystals of white tin (body-centered tetragonal structure) that abruptly transform into non-metallic gray tin (diamond structure) on cooling. These two forms of tin are called *allotropes*. Allotropes are also known for carbon, sulphur, phosphorous.

Binary and more complex compounds will usually stick to one type of bonding and differ only in their structural details, although these details are by no means unimportant. They can have major implications for observed properties. One usually distinguishes:

- *polymorphs* as different structural forms of the same chemical compounds. They are labeled with Greek letters: α-Sn, β-Sn, etc. Strictly speaking, allotropes can be also considered as polymorphs, as we just did for tin, and so all researchers do, especially

[16] The term *atomic radius* is somewhat more loosely defined, but most often it implies the covalent radius.

when they deal with high-pressure structures of elemental solids. The somewhat old-fashioned word "allotrope" is basically reserved for different forms of elemental solids observed at ambient pressure.

- *enantiomorphs* as left and right forms of a chiral structure (see Ch. 3.5)
- *polytypes* as different structures arising from different stacking sequences. Polytypes are common in layered structures like graphite, but they could also occur in structures derived from close-packed layers, as in Ch. 7.7. Labels of polytypes include the number of layers per unit cell and the indication of symmetry (cubic, hexagonal, rhombohedral). For example, zinc blende and wurtzite are the 3C- and 2H- polytypes of ZnS. Such polytypes are often observed in binary semiconductors.

8.4. van der Waals radius and Lennard-Jones potential

Coming to van der Waals crystals, one usually defines the *van der Waals radius* as an effective radius of an atom or molecule. Such radii appeared due to van der Waals who proposed an equation of state for non-ideal gas,

$$\left(p + \frac{a}{V^2}\right)(V - b) = RT \tag{8.2}$$

with the volume correction b that subtracts volumes of individual molecules from the total volume of the system.[17] Ironically, van der Waals never worked on the problem of chemical bonding (let alone on solids), but his concept of an effective radius proved very useful to identify main interactions between weakly bonded atoms or molecules. An appreciable van der Waals bonding occurs when the distance between atoms is less than the sum of the corresponding van der Waals radii. Any further contacts will of course lead to some minute bonding too, but it is even weaker than the aforementioned one and, to a first approximation, negligible.

The interactions in van der Waals crystals are usually described by an effective potential,

$$\mathcal{V}(r_{ij}) = -\frac{\mathcal{A}}{r_{ij}^6} + \frac{\mathcal{B}}{r_{ij}^{12}} \tag{8.3}$$

where $\mathcal{A}$ and $\mathcal{B}$ are constants, and r_{ij} is the distance between atoms. The first (attractive) term is due to London dispersion force between dipoles. The second (repulsive) term is an empirical potential akin to the one we used in Eq. (7.5). The power of 12 is chosen for reasons of mathematical convenience because this effective potential can be recast into the form

$$\mathcal{V}(r_{ij}) = 4\epsilon\left[-\left(\frac{\sigma}{r_{ij}}\right)^6 + \left(\frac{\sigma}{r_{ij}}\right)^{12}\right] \tag{8.4}$$

known as *Lennard-Jones potential*[18] with $\sigma = (\mathcal{B}/\mathcal{A})^{\frac{1}{6}}$ and $\epsilon = \mathcal{A}^2/4\mathcal{B}$.

8.5. Lattice energy

We will now repeat the same steps as in Ch. 7 to determine the equilibrium distance r_0 and the corresponding lattice energy. Total energy of a van der Waals crystal is determined by the summation of Eq. (8.4),

$$\mathcal{E}_{\text{tot}}(r) = \tfrac{1}{2}\sum_{i,j}\mathcal{V}(r_{ij}) = 2\epsilon\left[-A_6\left(\frac{\sigma}{r}\right)^6 + A_{12}\left(\frac{\sigma}{r}\right)^{12}\right] \tag{8.5}$$

[17] The constant a defines additional pressure caused by interactions between the molecules.

[18] We use σ and ϵ following the standard notation of the Lennard-Jones potential. They should not be confused with the stress and strain appearing in Ch. 9.

where r is the nearest-neighbor interatomic distance and we introduced lattice sums A_6 and A_{12}. They are similar in their meaning to the Madelung constant (Ch. 7.3), yet much easier to calculate because the series converge very fast. For an fcc crystal, $A_6 = 14.45$ and $A_{12} = 12.13$.

Setting the derivative of $\mathcal{E}_{\text{tot}}$ to zero yields the equilibrium distance,

$$\frac{d\mathcal{E}_{\text{tot}}}{dr} = 0 \;\Rightarrow\; 2\epsilon \left[\frac{6A_6}{r_0} \left(\frac{\sigma}{r_0} \right)^6 - \frac{12A_{12}}{r_0} \left(\frac{\sigma}{r_0} \right)^{12} \right] = 0 \;\Rightarrow\; r_0 = \sigma \left(\frac{2A_{12}}{A_6} \right)^{\frac{1}{6}} \tag{8.6}$$

that solely depends on the σ parameter of the potential. Then,

$$\mathcal{E}_{\text{lat}} = -\mathcal{E}_{\text{tot}}(r_0) = -2\epsilon \left[-A_6 \left(\frac{\sigma}{r_0} \right)^6 + A_{12} \left(\frac{\sigma}{r_0} \right)^{12} \right] = \epsilon \frac{A_6^2}{2A_{12}}, \tag{8.7}$$

so lattice energy solely depends on ϵ. This is certainly more elegant than the ionic case.

An interesting feature of van der Waals crystals is that they become more stable on increasing the lattice parameter. This is because $\mathcal{A}$ increases with the atomic radius, as the atoms become more polarizable. The $\mathcal{B}$ value should increase too to ensure the increase in $\sigma = (\mathcal{B}/\mathcal{A})^{\frac{1}{6}}$ and the lattice parameter, but $\epsilon = \mathcal{A}^2/4\mathcal{B}$ increases concurrently, because it contains $\mathcal{A}^2$. Larger atoms and molecules develop stronger van der Waals bonds. For example, melting points increase across the family of noble gases from neon to xenon, and likewise increase across halogens from F_2 to I_2. On the absolute scale, lattice energies of van der Waals crystal remain quite low, though, typically in the range of $10 - 200\,\text{meV/atom}$.

8.6. Bulk modulus

To calculate the bulk modulus, we repeat the procedure from Ch. 7.5. We will assume the fcc structure again, but now the atoms are at the lattice sites, so $r = a/\sqrt{2}$. Then volume per atom is $V = r^3/\sqrt{2}$ and

$$\frac{d}{dV} = \frac{\sqrt{2}}{3r^2} \frac{d}{dr}, \tag{8.8}$$

hence

$$B = V \frac{d^2\mathcal{E}_{\text{tot}}}{dV^2} = \frac{\sqrt{2}}{9\,r_0} \left. \frac{d^2\mathcal{E}_{\text{tot}}}{dr^2} \right|_{r=r_0} = \frac{4\epsilon}{\sigma^3} A_{12} \left(\frac{A_6}{A_{12}} \right)^{\frac{5}{2}}. \tag{8.9}$$

There is now the ratio of ϵ and σ^3, so the trend may be less intuitive than in the case of energy, but nevertheless bulk modulus of van der Waals crystals will typically increase with increasing the lattice parameter. Iodine is less compressible than solid bromine. The absolute values of the bulk modulus are typically below 10 GPa and even below 1 GPa for some of the lighter atoms and molecules.

9. Mechanical properties

Starting from this chapter, we will go through different crystal properties and discuss the main parameters that describe them. We will also see how these properties are related to microscopic aspects of the crystals, especially the atoms and their chemical bonding that constitute lattice degrees of freedom.

9.1. Hydrostatic pressure, Equation of state

Hydrostatic pressure implies that the same force acts on the sample from all directions. It is the type of pressure experienced by a sample immersed into water or another liquid. However, even liquids develop some pressure gradients. The most uniform pressure can be achieved by placing the crystal into helium gas. Helium solidifies at 11.5 GPa at room temperature, but it is a van der Waals solid with a very low bulk modulus, so it ensures almost hydrostatic (so-called *quasi-hydrostatic*) pressure conditions up to at least $20-25$ GPa.

Pressure renders chemical bonds more stiff, because atoms become closer to each other. Therefore, the bulk modulus increases on compression. One empirical (but very reasonable) approximation is linear pressure dependence of the bulk modulus,

$$B(p) = B_0 + B_0' p \tag{9.1}$$

where B_0 is the bulk modulus at ambient pressure and $B_0' = \text{const}$ is pressure derivative of the bulk modulus. Using this pressure dependence in Eq. (7.8) gives rise to a differential equation,

$$-V\frac{dp}{dV} = B_0 + B_0' p \;\Rightarrow\; \frac{dp}{B_0 + B_0' p} = -\frac{dV}{V} \tag{9.2}$$

that can be integrated to obtain the relation between p and V,

$$p(V) = \frac{B_0}{B_0'}\left[\left(\frac{V_0}{V}\right)^{B_0'} - 1\right]. \tag{9.3}$$

It is the *Murnaghan equation of state* that describes hydrostatic compression of crystals at low pressures $V/V_0 \geq 0.9$ where Eq. (9.1) holds. This equation of state describes the crystal at a constant temperature.

At higher pressures, a quadratic term should be added to Eq. (9.1), leading to the second-order Murnaghan equation of state. However, it is more common to use the so-called Birch-Murnaghan equations of state obtained by expanding free energy in powers of the strain (the step-by-step derivation can be found here). This equation can be second-, third-, or even higher order depending on how many terms in the expansion are retained. For the reference, we quote here the third-order *Birch-Murnaghan equation of state*, which is commonly used in geoscience,

$$p(V) = \frac{3B_0}{2}\left[\left(\frac{V_0}{V}\right)^{\frac{7}{3}} - \left(\frac{V_0}{V}\right)^{\frac{5}{3}}\right]\left[1 + \frac{3}{4}(B_0' - 4)\left(\left(\frac{V_0}{V}\right)^{\frac{2}{3}} - 1\right)\right]. \tag{9.4}$$

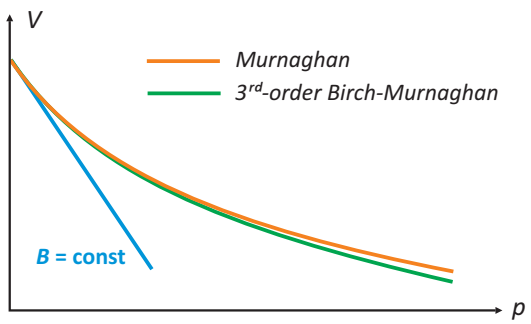

Figure 9.1: Pressure dependence of volume upon hydrostatic compression, according to the equations of state, (9.3) and (9.4).

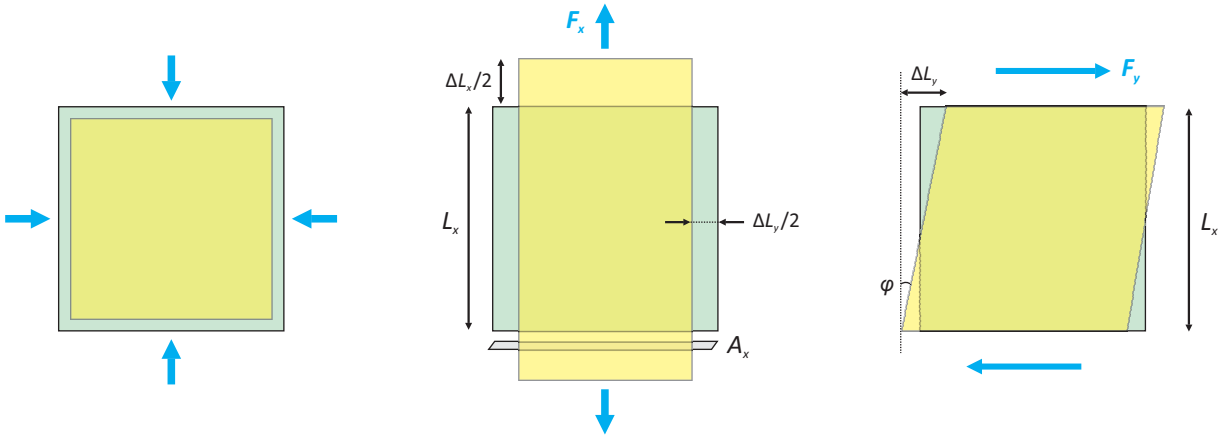

Figure 9.2: Hydrostatic compression (left), uniaxial pressure (middle), and shear deformation (right). Uniaxial strain is defined as $\epsilon_x = \Delta L_x/L_x$, whereas shear strain is defined as $\epsilon_{xy} = \tan\varphi \simeq \varphi$.

This equation contains the same three parameters as Eq. (9.3), but entails a different underlying approximation because no linear pressure dependence of B is assumed.

All equations of state show that volume decreases with pressure and develops a positive curvature, as shown in Fig. 9.1, because crystals harden on compression. Direct measurement of this $V(p)$ curve using *high-pressure XRD* (i.e., x-ray diffraction on a crystal placed into a pressure cell) is the main experimental tool for studying compressibility of solids and determining their bulk moduli.

9.2. Uniaxial pressure

In the absence of *pressure medium* like liquid or gas that could transmit the applied pressure into all directions and make it hydrostatic, one deals with *uniaxial pressure*. Such pressure is often called *stress*, $\sigma_x = F_x/A_x$ where F_x is the applied force and A_x is the area of the sample surface perpendicular to which this force is applied (Fig. 9.2, middle). Uniaxial stress creates *strain*, $\epsilon_x = \Delta L_x/L_x$, defined as the relative length change of the sample. Stress has units of pressure, whereas strain is a dimensionless quantity.

While it is difficult to expand the crystal hydrostatically, uniaxial pressure could either compress or stretch the crystal along a certain direction. One thus distinguishes between the *compressive* ($\epsilon > 0$) and *tensile* ($\epsilon < 0$) strains. Practically, uniaxial pressure can be created simply by squeezing the crystal between the two plates. However, more and more often piezo-devices are used instead. A suitably shaped crystal is attached to a piezoelectric stage that can create strains up to $1.5 - 2\%$, both compressive and tensile.

Stress and strain are related by the familiar *Hooke's law*,

$$\sigma_x = Y\epsilon_x \tag{9.5}$$

where Y is *Young's modulus*.

Uniaxial pressure changes not only the sample length, but also its aspect ratio. Squeezing the crystal along one direction will typically force it to expand along the perpendicular direction, and the other way around. This effect is gauged by the *Poisson's ratio*, $\nu = -\epsilon_y/\epsilon_x$. Most of the solid-state materials are characterized by $\nu > 0$. However, it is also possible to design materials with $\nu < 0$ known as *auxetic*. They play an important role in engineering, as explained here.

9.3. Shear deformation

Force can be applied not only perpendicular to the sample surface, but also parallel to it, leading to a so-called shear deformation that changes sample shape without changing its volume. Such shear stress $\tau_{xy} = F_y/A_x$ is defined in the same way as the uniaxial stress, whereas shear strain $\epsilon_{xy} = \Delta L_y/L_x = \tan\varphi$ is the relative displacement of the sample surface caused by F_y. For low displacements, $\tan\varphi \simeq \varphi$, and shear strain is measured simply as angle (Fig. 9.2, right).

The same linear relation between stress and strain holds in this case,

$$\tau_{xy} = G\,\epsilon_{xy}, \tag{9.6}$$

with the *shear modulus* G that complements B and E_Y in describing elastic properties of materials.

Up to this point we never referred to periodicity of the crystals. In fact, all of the above applies to any solid, be it crystalline or amorphous. In engineering, one often considers an isotropic medium, namely, a medium that shows the same behavior along all the directions. Such an isotropic medium is characterized by

$$E_Y = 3B(1-2\nu) = 2G(1+\nu). \tag{9.7}$$

Its elastic properties are then fully described by only two parameters. This is the case for a typical amorphous material like glass. Note however that Eq. (9.7) does not hold for crystals, because even cubic crystals are not isotropic. Their [100], [110], and [111] directions are distinct, as they are not related by any symmetry.

9.4. Stress and strain tensors

9.5. Elastic constants

General relation between stress and strain is set by the *elastic constants* C_{ijkl},

$$\sigma_{ij} = C_{ijkl}\,\epsilon_{kl}. \tag{9.8}$$

They have the same units of pressure (Pa) as all the elastic moduli. Elastic constants describe mechanical response of anisotropic media, including crystals. Technically, C_{ijkl} is a fourth-rank tensor (*elasticity tensor*) with 81 components, but symmetries of the stress and strain tensors allow several simplifications. Indeed, with only six independent components in σ and ϵ, respectively, it becomes convenient to introduce the aliases,

xx	yy	zz	xy	xz	yz
1	2	3	4	5	6

and consider 36 elastic constants from C_{11} to C_{66}.

Elastic constants can be also defined in a thermodynamic fashion as second derivatives of the elastic energy (energy acquired by the crystal due to its deformation),

$$\mathcal{E} = \mathcal{E}_0 + \frac{1}{2}\sum_{ij,kl} C_{ijkl}\,\epsilon_{ij}\,\epsilon_{kl}. \tag{9.9}$$

Mixed second derivatives are equal, so $C_{ijkl} = C_{klij}$ (see also Ch. 2.5), thus reducing the number of independent elastic constants to 21. Symmetry constrains them further. For example,

elasticity tensor of a cubic crystal takes the form

$$\mathbb{C} = \begin{pmatrix} C_{11} & C_{12} & C_{12} & 0 & 0 & 0 \\ C_{12} & C_{11} & C_{12} & 0 & 0 & 0 \\ C_{12} & C_{12} & C_{11} & 0 & 0 & 0 \\ 0 & 0 & 0 & C_{44} & 0 & 0 \\ 0 & 0 & 0 & 0 & C_{44} & 0 \\ 0 & 0 & 0 & 0 & 0 & C_{44} \end{pmatrix} \tag{9.10}$$

with only three independent parameters.

Inversion of the elasticity tensor yields the *compliance tensor*,

$$\epsilon_{ij} = S_{ijkl}\,\sigma_{kl}. \tag{9.11}$$

In Ch. 7 and 8, we saw that bulk modulus depends on the chemical bonding in crystals. Stronger bonds give rise to less compressible crystals. The same would be true for all the elastic constants. They are determined by the type of the crystal structure and the nature of chemical bonds.

Experimentally, elastic constants are determined from *resonant ultrasound spectroscopy*. Single crystal of the material is placed between two plates. Mechanical vibration is induced in one of these plates and transmitted to the opposite plate that shows vibrations at those frequencies where external modulation resonates with own frequencies of the crystal. These frequencies depend on the elastic constants of the material, but also on the shape and dimensions of the crystal. With the sufficient number of the resonant frequencies, all the 21 elastic constants can be determined and further measured as a function of temperature or other external parameters.

9.6. Plastic deformation

Instead of the ultrasound spectroscopy, engineers use *mechanical tests* where stress is applied to the sample and strain is measured, so that a *stress-strain curve* is obtained (Fig. 9.3). The initial, linear part of this curve yields one or another elastic modulus from Ch. 9.2 and 9.3. Such measurements will typically extend beyond the linear part of the curve until the regime of plastic deformation is reached. Whereas *elastic deformation* is reversible, *plastic deformation* remains in the sample after the stress is removed.

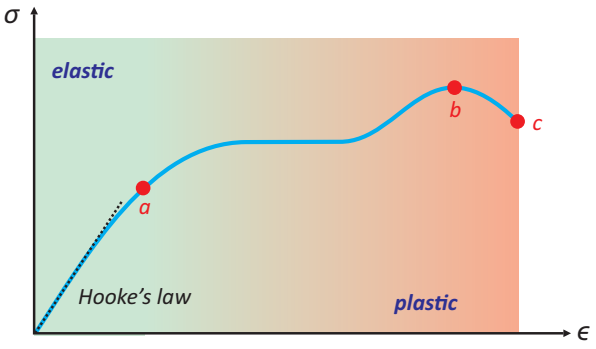

Figure 9.3: Stress-strain curve with the regions of elastic (reversible) and plastic (irreversible) deformation. Point a is the *yield point*, the onset of the plastic deformation. Point b shows the *ultimate strength* of the material. Point c indicates the *fracture* (breaking point).

Plastic deformation is characterized by a nonlinear regime of the stress-strain curve that starts at the so-called *yield point* and usually reaches a plateau where sample length keeps increasing without any additional stress applied. The material starts to "flow", similar to the heavily loaded plastic bag carried from the supermarket. This stretching region is followed by another increase (strain hardening) until the material reaches its point of *ultimate strength*. When this point is reached, a neck forms spontaneously even if no additional stress is applied, and eventually the sample breaks apart.

Materials characterized by a broad region of the plastic deformation are called *ductile*, in contrast to *brittle* materials that break close to the yield point. Ductility is usually defined with respect to tensile strain. The robustness of a material toward plastic deformation upon compressive or shear strain is called *malleability*. It is of crucial importance for metals and shows whether they can be rolled and bent. Finally, *hardness* is defined as the robustness of a material against indentation.

Microscopically, plastic deformations are related to the propagation of *dislocations*, linear defects that hinder periodicity of the crystal. The motion of dislocations shifts parts of the crystal relative to each other and increases the crystal length. Dislocations are especially abundant in metallic crystals where itinerant electrons are responsible for the chemical bonding, and relative positions of the atoms are less important. Therefore, metals, in contrast to the covalent and ionic crystals, are amenable to plastic deformations. On the other hand, alloys like steel where iron atoms are interspersed with carbon atoms, are less ductile because impurity atoms block the motion of dislocations.

Importantly, only elastic properties are intrinsic properties of the crystal, i.e., they are fully determined by the structure of the crystal, its constituent atoms and chemical bonds. On the other hand, ductility and other properties related to the plastic deformation are rooted in the microstructure, a combination of impurities and defects that affect the motion of dislocations.

10. Dielectric properties

10.1. Permittivity

Response to the external electric field $\mathbf{E}$ is described by *permittivity* (ε) of the crystal. This parameter shows the onset of the *electric polarization* $\mathbf{P}$ and of the corresponding *displacement field* $\mathbf{D}$,

$$\mathbf{D} = \varepsilon\varepsilon_0\mathbf{E} = \varepsilon_0\mathbf{E} + \mathbf{P}, \tag{10.1}$$

as local dipoles build up in the crystal and/or become aligned with the applied field.

Polarization is defined as the dipole moment per unit of volume, $P = n_d\mu_d$ where n_d is the dipole concentration and μ_d is the moment of a single dipole. P has the units of C/m^2 and also serves as a measure of charge per area, but one should remember that this charge is always compensated by the same charge of the opposite sign sitting somewhere else in the crystal.

It is also customary to define *dielectric susceptibility*,

$$\chi_e = \frac{P}{\varepsilon_0 E} \qquad \Rightarrow \qquad \varepsilon = 1 + \chi_e. \tag{10.2}$$

Both ε and χ_e are 3×3 tensors[19] that reduce to scalars in cubic crystals.

Both dielectric susceptibility and permittivity are frequency-dependent complex numbers. One typically separates them into the real and imaginary parts,

$$\varepsilon(\omega) = \varepsilon' + i\varepsilon'' \qquad \text{and} \qquad \chi_e(\omega) = \chi_e' + i\chi_e'' \tag{10.3}$$

that show, respectively, the polarization in-phase and out-of-phase with the oscillating electric field, $E = E_0\, e^{-i\omega t}$. Indeed,

$$P = \chi_e' E_0\, e^{-i\omega t} + \chi_e'' E_0\, ie^{-i\omega t} = (\varepsilon' - 1)E_0\, e^{-i\omega t} + \varepsilon'' E_0\, ie^{-i\omega t}. \tag{10.4}$$

At low frequencies, ε' approaches static permittivity $\varepsilon_{\rm st}$, whereas ε'' vanishes. At high frequencies, ε' approaches 1 (vacuum permittivity), because electric field oscillates too fast to induce any polarization, and ε'' again vanishes.

10.2. Dielectric loss

Complex permittivity shows the energy loss (heating) of a dielectric in oscillating electric fields. Consider Maxwell's equation (A.4) that in the absence of the magnetic field can be represented as,

$$\boldsymbol{j} = -\frac{\partial \mathbf{D}}{\partial t} = -\varepsilon_0\omega\,(i\varepsilon' - \varepsilon'')\,\mathbf{E} = \boldsymbol{j}_\perp + \boldsymbol{j}_\parallel. \tag{10.5}$$

No electric current flows through the dielectric, but there is an instantaneous local current generated by dipoles that move in order to get aligned with the applied field. This "dipole current" comprises two components, which are perpendicular and parallel to the field, respectively. Joule heating is given by $\mathbf{E}\cdot\boldsymbol{j}$, so only ε'' ($\boldsymbol{j}_\parallel$) is responsible for the heating.

The imaginary permittivity (ε'') is often called *dielectric loss*. One also defines the *loss tangent*,

$$\tan\delta = \frac{\varepsilon''}{\varepsilon'} = \frac{|\boldsymbol{j}_\parallel|}{|\boldsymbol{j}_\perp|} \tag{10.6}$$

with the *loss angle* δ. The loss tangent and loss angle show how much heat is produced by a dielectric placed into an oscillating electric field. Materials with low dielectric loss are required

[19] In the general case, χ_e is the derivative of $\mathbf{P}$ with respect to $\mathbf{E}$.

in power applications to avoid heating by the ac-field. On the other hand, commercial microwave ovens are tuned to the frequency that renders the large dielectric loss in water. Therefore, food can be microwaved and heated, whereas its container remains cold.

10.3. Induced dipoles and polarizability

Local dipoles in dielectrics can be divided into two groups, *permanent* and *induced*. Permanent dipoles occur in polar molecules and crystals. They carry some dipole moment that can be turned by the applied electric field, resulting in *orientation polarization*. By contrast, induced dipoles arise from the polarization of those atoms and molecules that would remain nonpolar in the absence of the applied field. One prominent example of this mechanism is the *ionic polarization* due to an optical phonon (Ch. 12).

Induced dipole moments are proportional to the electric field,

$$\boldsymbol{\mu}_d = \alpha\, \mathbf{E}_{\text{local}} \tag{10.7}$$

where α is *polarizability* (again, tensor property that in lucky cases can be reduced to a scalar). This definition is quite tricky because it involves local electric field near the atom/molecule, which is generally different from the applied electric field. We will deal with this problem shortly. For now let's notice that polarizability has rather non-intuitive SI units of $\mathrm{C\,m^2/V}$ or $\mathrm{F\,m^2}$. It becomes much more palatable in electrostatic CGS units [$\varepsilon_0 = 1/(4\pi)$] where α is measured in $\mathrm{cm^3}$ and corresponds to an effective volume of an atom/molecule.

10.4. Local electric field

Local electric field from Eq. (10.7) includes three contributions (Fig. 10.1),

$$\mathbf{E}_{\text{local}} = \mathbf{E}_{\text{ext}} + \mathbf{E}_{\text{depol}} + \mathbf{E}_L. \tag{10.8}$$

One is the external field $\mathbf{E}_{\text{ext}}$, the second one is the depolarizing field $\mathbf{E}_{\text{depol}}$ arising from charges that accumulate on the surface, and the third one is the Lorentz field $\mathbf{E}_L$ due to charges in the interior of the dielectric. The first two terms, $\mathbf{E} = \mathbf{E}_{\text{ex}} + \mathbf{E}_{\text{depol}}$, build up the electric field used in Maxwell's equations.

One good thing about $\mathbf{E}_{\text{depol}}$ and $\mathbf{E}_L$ is that they are proportional to polarization, because both fields arise from charges inside the dielectric and on its surface. The *depolarizing field* depends on the sample shape,

$$\mathbf{E}_{\text{depol}} = -f\,\frac{\mathbf{P}}{\varepsilon_0}, \tag{10.9}$$

where f is the *depolarization factor*, basically a form factor. Its calculation is a rather tedious exercise in electrostatics that, reportedly, Landau gave to his students as one problem of the "theory minimum". Less ambitious students should be alright with the simple knowledge that flat sample features $f = 1$ because a lot of charge is accumulated on its surfaces, and it acts as a capacitor of some sort. By contrast, needle-like sample features $f = 0$. Spherical sample is somewhat in between with its $f = \frac{1}{3}$, as we will see shortly.

Lorentz field arises from charges in the interior of the dielectric. Envisage a small spherical hole that has been cut out inside the sample. The charge accumulated on this new surface produces electric field in the center of the sphere and acts opposite to the depolarizing field. We introduce spherical coordinates with the polar angle θ that gauges the angle with respect to $\mathbf{E}$. We then slice the sphere perpendicular to the direction of $\mathbf{E}$, such that each slice is a ring with the radius $R\sin\theta$ and thickness $R\,d\theta$ (Fig. 10.1, right). The polarization is maximum in

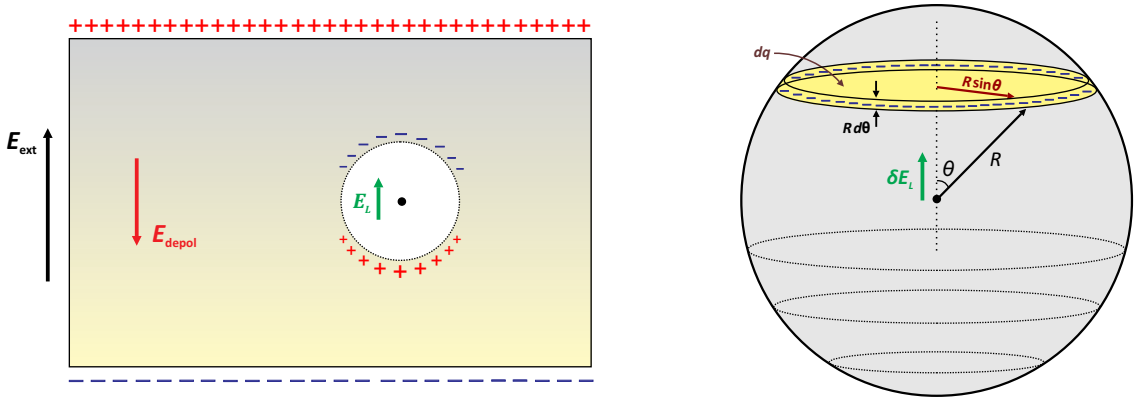

Figure 10.1: Left: local electric field is obtained as a superposition of the external field $\mathbf{E}_{\rm ext}$, depolarizing field $\mathbf{E}_{\rm depol}$ produced by charges on the surface, and Lorentz field $\mathbf{E}_L$ produced by charges in the interior of the dielectric. Right: calculation of the Lorentz field by slicing the sphere and evaluating the electric field δE_L created by each slice in its center.

the zenith and minimum at $\theta = \pi/2$, hence for a given slice $P(\theta) = -P\cos\theta$, and the overall charge on the slice is polarization times area, namely,

$$\delta q = -P\cos\theta \times 2\pi R\sin\theta \times Rd\theta = -2\pi R^2 P \sin\theta\cos\theta\, d\theta. \tag{10.10}$$

Electric field imposed by such a ring is

$$\delta E_L = -\frac{1}{4\pi\varepsilon_0}\frac{\delta q}{R^2}.$$

The components perpendicular to $\mathbf{E}$ cancel, whereas those parallel to $\mathbf{E}$ contribute to the overall field created by the ring. Therefore, we should take the projection of δE_L, which adds the factor of $\cos\theta$, resulting in

$$\delta E_L^{\parallel} = -\frac{1}{4\pi\varepsilon_0}\frac{\delta q}{R^2}\cos\theta = \frac{P}{2\varepsilon_0}\cos^2\theta\sin\theta\, d\theta \tag{10.11}$$

for the electric field produced by the ring. We are left to integrate this over θ,

$$\mathbf{E}_L = \frac{\mathbf{P}}{2\varepsilon_0}\int_0^{\pi}\cos^2\theta\sin\theta\, d\theta = \frac{\mathbf{P}}{2\varepsilon_0}\int_{-1}^{1}\cos^2\theta\, d(\cos\theta) = \frac{\mathbf{P}}{2\varepsilon_0}\frac{\cos^3\theta}{3}\bigg|_{-1}^{1} = \frac{\mathbf{P}}{3\,\varepsilon_0}. \tag{10.12}$$

This calculation also elucidates the depolarization factor of $f = \frac{1}{3}$ for the sphere.

10.5. Clausius-Mossotti relation

Induced dipole moments depend on the local field that, in turn, depends on the polarization created by these dipoles. Therefore, *microscopic* polarizability of atoms/molecules is directly related to the *macroscopic* permittivity of the sample. Consider $\mathbf{E}_{\rm local} = \mathbf{E} + \mathbf{E}_L$ and use it in the definition of the polarization. One one hand,

$$\mathbf{P} = n_d\mu_d = n_d\alpha\mathbf{E}_{\rm local} = n_d\,\alpha\left(\mathbf{E} + \frac{\mathbf{P}}{3\,\varepsilon_0}\right). \tag{10.13}$$

On the other hand,

$$\mathbf{P} = \chi_e\varepsilon_0\mathbf{E} = (\varepsilon - 1)\varepsilon_0\mathbf{E}. \tag{10.14}$$

By evaluating $\mathbf{E}$ and canceling $\mathbf{P}$, one finds

$$\frac{\varepsilon - 1}{\varepsilon + 2} = \frac{\chi_e}{3 + \chi_e} = \frac{n_d\,\alpha}{3\varepsilon_0}, \tag{10.15}$$

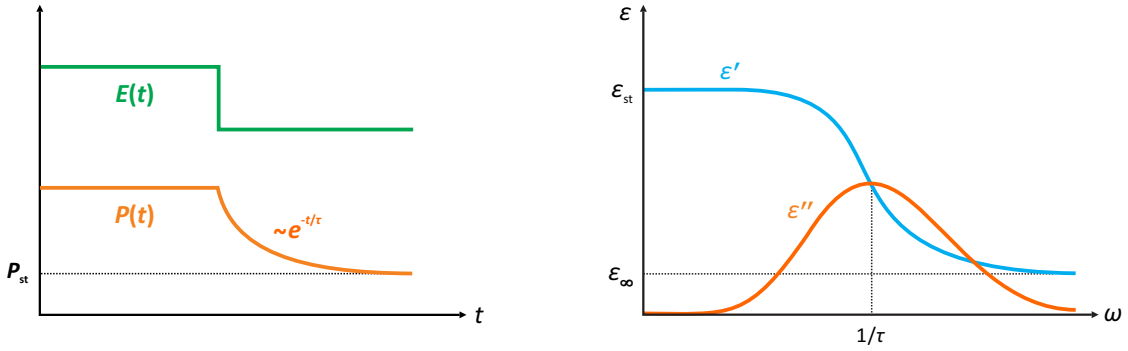

Figure 10.2: Debye model of relaxation. Left: an abrupt change in the electric field E gives rise to an exponential change of the polarization with the single relaxation time τ. Right: real and imaginary parts of the permittivity as a function of frequency.

the *Clausius-Mossotti relation*, also known as the *Lorentz-Lorenz equation*. Simple at first glance, it has been very significant historically, because it offered the very first experimental tool for probing molecular property (polarizability) using a macroscopic measurement (permittivity).

10.6. Permanent dipoles, Debye relaxation

Let's now consider permanent dipoles. To a first approximation, they do not change their dipole moment, yet they turn in order to get aligned with the field. This rotation takes time and causes a delay between $\mathbf{P}$ and $\mathbf{E}$, hence the imaginary part of ε. To analyze this delay, consider first a simple situation when external electric field is changed abruptly. We assume exponential nature of the relaxation with the characteristic *relaxation time* τ (Fig. 10.2), such that

$$P(t) = P_{\rm st}\left(1 + e^{-t/\tau}\right) \quad \Rightarrow \quad \frac{dP}{dt} = -\frac{P(t) - P_{\rm st}}{\tau} \tag{10.16}$$

where $P_{\rm st} = \varepsilon_0 \chi_0 E$ is the static polarization reached at $t \to \infty$ assuming that the field does not change.

Using the standard ansatz $P(t) = P_0\, e^{-i\omega t}$, we find

$$P_0 = \frac{\varepsilon_0 \chi_0 E_0}{1 - i\omega\tau} \quad \Rightarrow \quad \chi_e = \frac{P}{\varepsilon_0 E} = \frac{\chi_0}{1 - i\omega\tau}, \tag{10.17}$$

the Debye relaxation. It is a standard form of a response function for a system with the single relaxation time. We will see it again when we come to discuss ac-conductivity of metals (Ch. **??**). For now, let's get more familiar with the expressions. Using $\chi = \chi' + i\chi''$, one finds

$$\chi_e'(\omega) = \frac{\chi_0}{1 + \omega^2\tau^2}, \quad \chi_e''(\omega) = \frac{\chi_0\, \omega\tau}{1 + \omega^2\tau^2}, \tag{10.18}$$

where χ_0 is static susceptibility.

We can also use Eq. (10.2) to calculate permittivity,

$$\varepsilon'(\omega) = 1 + \frac{\varepsilon_{\rm st} - 1}{1 + \omega^2\tau^2}, \quad \varepsilon''(\omega) = \frac{(\varepsilon_{\rm st} - 1)\, \omega\tau}{1 + \omega^2\tau^2}, \tag{10.19}$$

with the static permittivity $\varepsilon_{\rm st} = 1 + \chi_0$. The imaginary component $\varepsilon''(\omega)$ has a peak-like structure with the maximum at $\omega\tau = 1$, i.e., at a characteristic relaxation frequency determined by the relaxation time τ (Fig. 10.2). It is the target frequency if we want to maximize dielectric

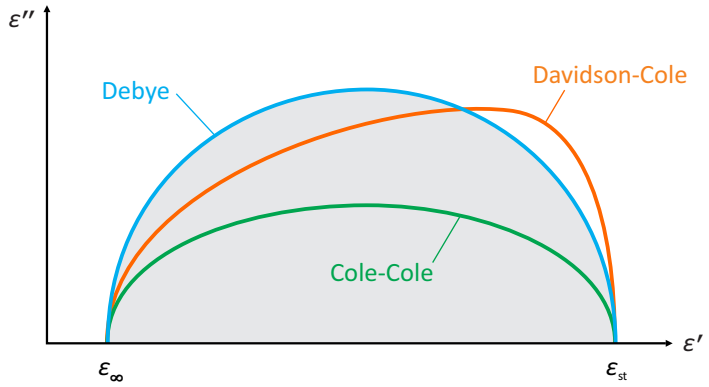

Figure 10.3: Dielectric relaxation represented by the Cole-Cole plot. Debye relaxation (single value of τ) manifests itself by a semi-circle. The Cole-Cole and Davidson-Cole models describe dielectrics with multiple relaxation times.

loss and heat the sample by microwave radiation.[20] The real part ε' equals static permittivity at $\omega = 0$ and decays to 1 at $\omega \to \infty$.

Debye relaxation occurs at frequencies determined by the value of τ. Liquids feature relaxation times on the order of picoseconds and the $\varepsilon''(\omega)$ peak in the GHz range. In solids, dipoles are more constrained, so their relaxation time increases to milliseconds, whereas the peak shifts into the kHz range. All of these frequencies are anyway much lower than typical phonon frequencies, which lie in the THz range. In fact, Debye relaxation is never the only process induced by the oscillating electric field, and $\varepsilon'(\omega)$ never reaches 1 at high frequencies (see also Ch. 12). This aspect is taken into account by the modified expression where we introduced the high-frequency limit ε_∞,

$$\varepsilon(\omega) = \varepsilon_\infty + \frac{\varepsilon_{\rm st} - \varepsilon_\infty}{1 + i\omega\tau}. \tag{10.20}$$

Here, "high frequency" means the frequency well above the frequency $\omega = 1/\tau$ of the Debye relaxation.

10.7. Cole-Cole plots

In practical dielectric measurements, one seeks to determine the relaxation time(s) of the system. To this end, *Cole-Cole plots* of ε'' vs. ε' with ω as an implicit parameter are commonly used. Debye relaxation gives rise to the semicircular Cole-Cole plot, because all points defined by Eq. (10.20) lie on the semi-circle centered at $(\varepsilon_{\rm st} + \varepsilon_\infty)/2$ and having the radius of $(\varepsilon_{\rm st} - \varepsilon_\infty)/2$, see Fig. 10.3.

The model of Debye relaxation works well for liquids like water or ethanol. In more complex cases, and especially in mixtures of liquids, multiple relaxation times may be present, and the semi-circle becomes deformed. Some common approximations in this case are the *Cole-Cole equation*,

$$\hat{\varepsilon}(\omega) = \varepsilon_\infty + \frac{\varepsilon_{\rm st} - \varepsilon_\infty}{1 + (i\omega\tau)^{1-\alpha}}, \tag{10.21}$$

and the *Davidson-Cole equation*,

$$\hat{\varepsilon}(\omega) = \varepsilon_\infty + \frac{\varepsilon_{\rm st} - \varepsilon_\infty}{(1 + i\omega\tau)^{\beta}}. \tag{10.22}$$

Needless to say, α and β can be used at the same time, thus leaving even more flexibility. The Cole-Cole equation renders the ε'' vs. ε' graph non-circular, while keeping the symmetry with respect to the mid-point at $(\varepsilon_{\rm st} - \varepsilon_\infty)/2$. In contrast, the Davidson-Cole relaxation leads to a semi-circle stretched on one side and suppressed on the other (Fig. 10.3). The Cole-Cole plots

[20] Commercial microwave ovens operate at 2.4 GHz, which is somewhat away from the peak of $\varepsilon''(\omega)$ for water, in order to avoid overheating.

are widely used for analyzing relaxation behavior based on frequency-dependent measurements, not only in dielectrics but also for example in spin glass.

11. Phonons and sound

11.1. Underlying approximations

Atomic motion determines many, if not all, properties of a crystal. Molecules show characteristic vibrations (normal modes) that occur at special frequencies. Crystals feature collective atomic vibrations too, but their nature is somewhat more involved than in the case of molecules. To understand these vibrations in the simplest possible way, we will take advantage of several approximations:

- *classical*, namely, we will treat atomic motion using classical mechanics and obtain *displacement waves* that describe collective atomic motion in the crystal. Quantum mechanics requires this motion to be quantized. The corresponding quantum is called *phonon*, but we usually do not need to solve the respective problem on the quantum level. It is sufficient to quantize the waves obtained classically, as we will consciously do in Ch. **??**.
- *harmonic*, namely, elastic energy is quadratic in the displacement, or in other words any displacement creates a restoring force, which is proportional to the displacement. Harmonic approximation works well most of the time, although in Ch. **??** we will see the need to go beyond it.
- *adiabatic*, namely, atomic (nuclear) and electronic degrees of freedom are separated from each other. This is possible because nuclei are much heavier than electrons, so electrons move a lot faster. One can then think of electrons as creating a potential energy landscape for the nuclear motion. The typical time scale of electronic and nuclear motion is 10^{-15} s and 10^{-12} s, respectively. This approximation is also known as the *Born-Oppenheimer approximation*, especially in the context of molecules. It goes back to the very general adiabatic theorem of quantum mechanics. The adiabatic approximation fails when two different electronic states have similar energies, and nuclei no longer know in which potential energy landscape to move. Such cases are fairly rare in the ground state,[21] yet they become more common when excited electronic states are considered, for example, when crystal is hit by a laser that drives an electronic excitation of some sort.

11.2. Monoatomic chain

Let's consider the simplest possible case, a chain of atoms with equal spacings a. We will use the index p to label atoms along this chain, and introduce the atomic displacements u_p (Fig. 11.1). Any displacement changes the interatomic distance, and we will assume that chemical bonds behave as springs with the stiffness $\mathcal{K}$. The overall elastic energy is then

$$\mathcal{E}_{\text{elastic}} = \frac{1}{2}\sum_p \mathcal{K}(u_{p+1} - u_p)^2. \tag{11.1}$$

Atomic displacements can be determined from the equations of motion,

$$m\frac{d^2u_p}{dt^2} = -\frac{\partial \mathcal{E}_{\text{elastic}}}{\partial u_p} = -\mathcal{K}(2u_p - u_{p+1} - u_{p-1}). \tag{11.2}$$

where m is the atomic mass. Instead of trying a brute force solution of these coupled differential equations, we will choose an ansatz,

$$u_p(t) = e^{i(qpa-\omega t)} \tag{11.3}$$

[21] But by all means not impossible, see the Jahn-Teller effect.

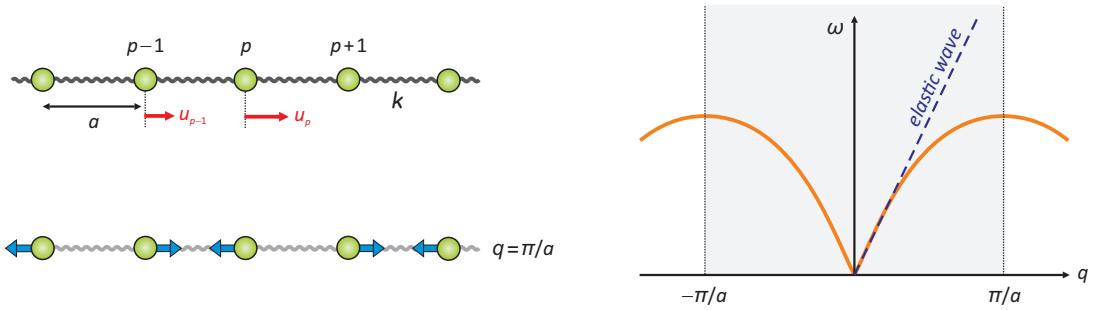

Figure 11.1: Atomic displacements u_p in the monoatomic chain. The right panel shows the dispersion relations for the displacement wave (orange) and elastic wave (blue). The light-blue arrows indicate the atomic displacements at $q = \pi/a$.

that essentially describes oscillations with the frequency ω that propagate along the chain with the propagation vector q (we consider the 1D situation, so the scalar suffices). The first part, e^{iqpa}, is basically a phase shift between the oscillations of different atoms.

Using Eq. (11.3) in Eq. (11.2), one finds $-m\omega^2 = -\mathcal{K}(2 - e^{iqa} - e^{-iqa})$ and

$$\omega^2(q) = 2\frac{\mathcal{K}}{m}\left[1 - \cos(qa)\right] \;\Rightarrow\; \omega(q) = 2\sqrt{\frac{\mathcal{K}}{m}} \times \left|\sin\frac{qa}{2}\right| \tag{11.4}$$

where we used the absolute value because frequency must be positive. This is a *dispersion relation* for the displacement wave (phonon) in a monoatomic chain. One immediately notices that $\omega(q)$ is symmetric with respect to $q = 0$ and shows periodicity of $2\pi/a$ (Fig. 11.1) that intriguingly matches periodicity of the reciprocal lattice (Ch. 5.2). Full implications of this fact will become clear in Ch. 13. For now we will stay away from it and analyze the dispersion relation. By definition, the value of q shows the phase shift between the displacements of neighboring atoms. When this phase shift is small, springs stretch very little, and the wave energy (hence frequency) is low. It increases with increasing q. At $q = \pi/a$, the phase shift becomes π, so adjacent atoms move opposite to each other, thus forming a standing wave (Fig. 11.1).

At low q, one can use $\sin(qa/2) \simeq qa/2$ and write the linear dispersion relation

$$\omega(q) = a\sqrt{\frac{\mathcal{K}}{m}} \times q \tag{11.5}$$

that corresponds to the group velocity of

$$v_{\text{ph}} = \frac{d\omega}{dq} = a\sqrt{\frac{\mathcal{K}}{m}} \tag{11.6}$$

This is the speed of sound, as we will see shortly.

11.3. Elastic waves and sound

Sound is an elastic wave that propagates in any compressible medium. Consider a bar with the cross-section A subject to a deformation that leads to the displacement $u_x(x)$ of the volume element $A\,dx$ parallel to the bar (Fig. 11.2). Time dependence of the displacement is described by the usual equation of motion,

$$m\frac{\partial^2 u_x}{\partial t^2} = \sum F = F(x + dx) - F(x) \tag{11.7}$$

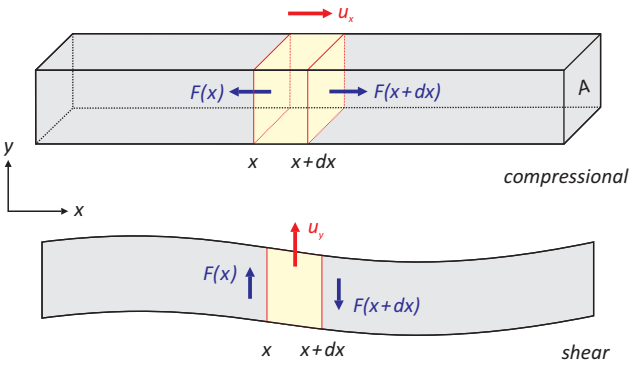

Figure 11.2: Compressional and shear elastic waves. The forces $F(x)$ and $F(x+dx)$ cause the displacements u_x and u_y along the bar and perpendicular to the bar, respectively.

where forces act on both sides of the volume element. By introducing volume density $\rho = m/V$, one can write

$$(\rho A\, dx)\,\frac{\partial^2 u_x}{\partial t^2} = F(x+dx) - F(x) \;\Rightarrow\; \rho\,\frac{\partial^2 u_x}{\partial t^2} = \frac{1}{A}\frac{\partial F}{\partial x} = \frac{\partial \varsigma_{xx}}{\partial x} \tag{11.8}$$

Hooke's law relates stress and strain, $\varsigma_{xx} = Y\epsilon_{xx}$ via the Young's modulus Y, whereas strain can be represented as $\epsilon_{xx} = \partial u_x/\partial x$, so overall

$$\frac{\partial^2 u_x}{\partial t^2} = \frac{Y}{\rho} \times \frac{\partial^2 u_x}{\partial x^2}. \tag{11.9}$$

This is the standard wave equation solved by our earlier ansatz, Eq. (11.3), but with the dispersion relation

$$\omega^2 = v_s^2\, q^2 \quad \text{where} \quad v_s = \sqrt{\frac{Y}{\rho}}. \tag{11.10}$$

The speed v_s resembles our earlier result, Eq. (11.6) obtained in the $q \to 0$ limit, and serves as the *speed of sound*.

An important difference between the compressional elastic wave in a continuous medium, as we considered here, and the displacement wave in a crystal (Ch. 11.2) is that linear dispersion relation, $\omega = v_s\, q$, breaks down in the latter at higher q's (Fig. 11.1). This happens because crystal is discrete, so it can't be treated as a continuous medium when period of the displacement wave becomes comparable to the interatomic distance or, in other words, q approaches π/a. However, the continuum approximation is perfectly justified at low q's where period of the displacement wave is large compared to the interatomic distance. Continuum approximations are widely used in solid-state physics for describing mesoscopic phenomena, for example long-period spin textures and magnetic skyrmions.

We can also envisage a wave of displacements u_y, which are perpendicular to the bar (Fig. 11.2). The solution is similar to the previous case and involves the shear stress, $\tau_{xy} = F/A$, as well as the shear strain, $\epsilon_{xy} = \partial u_y/\partial x$, related by $\tau_{xy} = G\,\epsilon_{xy}$ with the shear modulus G. The resulting wave equation,

$$\frac{\partial^2 u_y}{\partial t^2} = \frac{G}{\rho} \times \frac{\partial^2 u_y}{\partial x^2}, \tag{11.11}$$

describes a *shear wave* propagating with the velocity of $\sqrt{G/\rho}$.

Compressional wave propagates in any elastic medium, whereas shear waves only propagate in solids because gases and liquids feature $G = 0$ (their shape can be changed at no energy cost). This is the main reason why sound is a compressional wave. Shear wave can be thought as sound too, but it's not audible because our hearing mechanism involves sound transmission through air.

11.4. Longitudinal and transverse phonons

The phonon described in Ch. 11.2 is called *acoustic* because $q \to 0$ part of its dispersion relation describes sound propagation in crystals. A similar acoustic phonon with displacements perpendicular to the propagation direction exists too. Different names can be used to describe these two types of motion depending on the context,

acoustic phonon	longitudinal	transverse
elastic wave	compressional	shear
seismic wave	p-wave	s-wave

Speeds of the corresponding waves are given by

$$v_{\mathrm{LA}} = \sqrt{\frac{B + \frac{4}{3}G}{\rho}}, \qquad v_{\mathrm{TA}} = \sqrt{\frac{G}{\rho}} \tag{11.12}$$

which are, for example, velocities of the primary (p) and secondary (s) seismic waves. Since $v_{\mathrm{LA}} > v_{\mathrm{TA}}$, p-wave always arrives earlier than s-wave. This time delay measured by a seismometer gauges the distance to the epicentre of an earthquake. Likewise, the data on the propagation of p-waves and s-waves provides information on the internal structure of Earth. The existence of the liquid outer core and inner solid core is inferred from the refraction of p-waves and from the fact that s-waves do not reach points on the opposite side of Earth, because shear waves do not propagate through liquid.

In Eq. (11.12), v_{TA} is equal to the velocity of the shear wave as determined in Ch. 11.3. However, v_{LA} is different from the velocity of the compressional wave in a thin bar, because Poisson's ratio should be taken into account in a 3D solid.

In liquid and gas, $G = 0$ and speed of sound is described by the *Newton-Laplace equation*,

$$v = \sqrt{\frac{B}{\rho}} \tag{11.13}$$

11.5. Diatomic chain

Let us now extend this analysis to a diatomic chain with alternating atoms and equal separations, such that all bonds have the same stiffness $\mathcal{K}$. We will proceed similar to the previous case and consider atomic displacements propagating along the chain, but now the two atoms have different mass and should thus show different displacement amplitudes,

$$u_p(t) = A_1\, e^{i(qpa - \omega t)}, \qquad v_p(t) = A_2\, e^{i(qpa - \omega t)}. \tag{11.14}$$

The equations of motion become

$$\begin{aligned} m_1 \frac{d^2 u_p}{dt^2} &= -\mathcal{K}(u_p - v_p) - \mathcal{K}(u_p - v_{p-1}), \\ m_2 \frac{d^2 v_p}{dt^2} &= -\mathcal{K}(v_p - u_p) - \mathcal{K}(v_p - u_{p+1}). \end{aligned}$$

Our ansatz for u_p and v_p returns a system of two linear equations for the amplitudes A_1 and A_2,

$$\begin{cases} -m_1\omega^2 A_1 = -\mathcal{K}A_1 + \mathcal{K}A_2 - \mathcal{K}A_1 + \mathcal{K}A_2\, e^{-iqa} \\ -m_2\omega^2 A_2 = -\mathcal{K}A_2 + \mathcal{K}A_1 - \mathcal{K}A_2 + \mathcal{K}A_1\, e^{iqa} \end{cases}$$

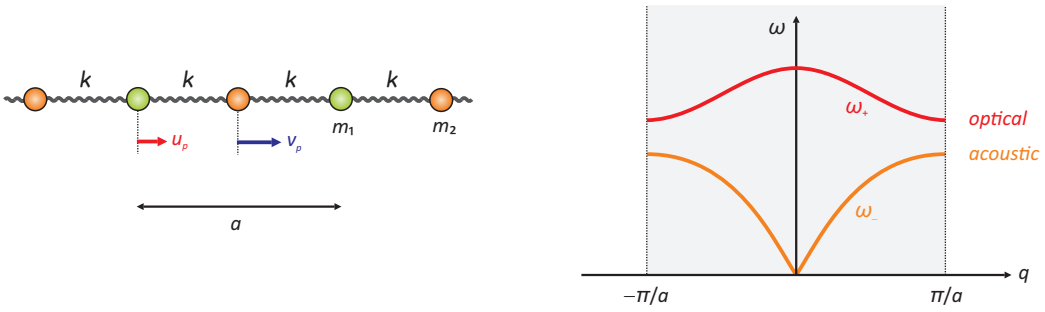

Figure 11.3: Left: atomic displacements in the diatomic chain comprising atoms with the masses m_1 and m_2 connected by the springs with the same stiffness $\mathcal{k}$. Right: dispersion relation for the two phonon modes, acoustic and optical.

or

$$\begin{cases} (m_1\omega^2 - 2\mathcal{k})A_1 + \mathcal{k}(1 + e^{-iqa})A_2 = 0 \\ \mathcal{k}(1 + e^{iqa})A_1 + (m_2\omega^2 - 2\mathcal{k})A_2 = 0 \end{cases} \tag{11.15}$$

The solution for A_1 and A_2 exists when the determinant is zero, namely,

$$\begin{vmatrix} m_1\omega^2 - 2\mathcal{k} & \mathcal{k}(1 + e^{-iqa}) \\ \mathcal{k}(1 + e^{iqa}) & m_2\omega^2 - 2\mathcal{k} \end{vmatrix} = 0 \tag{11.16}$$

This condition returns a quadratic equation for ω^2,

$$m_1 m_2\, \omega^4 - 2\mathcal{k}(m_1 + m_2)\, \omega^2 + 2\mathcal{k}^2[1 - \cos(qa)] = 0, \tag{11.17}$$

and

$$\omega^2(q) = \frac{\mathcal{k}}{m} \pm \mathcal{k}\sqrt{\frac{1}{m^2} - \frac{4}{m_1 m_2}\sin^2\frac{qa}{2}} \tag{11.18}$$

where we introduced the *reduced mass*,

$$\frac{1}{m} = \frac{1}{m_1} + \frac{1}{m_2} \tag{11.19}$$

11.6. Acoustic and optical phonons

There are now two dispersion relations that define two *phonon branches*. The $\omega_-(q)$ branch has zero frequency at $q = 0$. It is called *acoustic* because it reduces to an elastic wave in the low-q limit and describes sound propagation. The $\omega_+(q)$ branch is *optical*, because it can interact with light, as we will see in Ch. 12. Optical phonon has the finite frequency of $\sqrt{2\mathcal{k}/m}$ at $q = 0$.

The main intrinsic difference between the acoustic and optical phonons lies in the amplitudes A_1 and A_2. For an optical branch at $q = 0$, Eqs. (11.15) yield $A_1/A_2 = -m_2/m_1$. The atoms of different type oscillate out-of-phase. On the other hand, $\omega_- = 0$ of the acoustic mode yields $A_1/A_2 = 1$, such that atoms of different type oscillate in-phase near $q = 0$.

At $q = \pi/a$, one finds $\omega_+ = \sqrt{2\mathcal{k}/m_2}$ and $\omega_- = \sqrt{2\mathcal{k}/m_1}$ when $m_1 > m_2$. Then,

$$\left(\frac{A_1}{A_2}\right)_+ = -\frac{\mathcal{k}(1 + e^{-iqa})}{m_1\omega_+^2 - 2\mathcal{k}} \to 0, \qquad \left(\frac{A_1}{A_2}\right)_- = -\frac{m_2\omega_-^2 - \mathcal{k}}{\mathcal{k}(1 + e^{iqa})} \to \infty. \tag{11.20}$$

It means that only the light atoms (m_2) oscillate in the optical mode, whereas only the heavy atoms (m_1) oscillate in the acoustic mode. A nice visualization of the modes at arbitrary q-values and for different m_2/m_1 ratios can be found here.

12. Phonons and light

Whereas acoustic phonons are responsible for propagation of sound, optical phonons interact with light. To understand this interaction, we will first review the meaning of optical constants and then derive optical reflectivity of an ionic crystal due to phonons.

12.1. Refractive index and reflectivity

Optical response of a material (solid, liquid, or gas) is determined by its *refractive index*. The refractive index n appears in the dispersion relation of an electromagnetic wave (Ch. A.2),

$$\varepsilon\,\omega^2 = c^2k^2 \quad \text{with} \quad \varepsilon = n^2 \tag{12.1}$$

where ε is permittivity, k is the length of the propagation vector, and $c = 3\times10^8\,\mathrm{m/s}$ is speed of light in vacuum. Since ε is generally a complex number, n is a complex number too, $n = n' + in''$.[22] Using $\mathbf{k} = (n/c)\,\omega = n\,\mathbf{k}_0$, one writes the oscillating electric field as

$$\mathbf{E} = \mathbf{E}_0\,e^{i(\mathbf{kr}-\omega t)} = \mathbf{E}_0\,e^{i(n\mathbf{k}_0\mathbf{r}-\omega t)} = \mathbf{E}_0\,e^{-n''\mathbf{k}_0\mathbf{r}}\,e^{i(n'\mathbf{k}_0\mathbf{r}-\omega t)} \tag{12.2}$$

where $\mathbf{k}_0$ is the propagation vector in vacuum ($\varepsilon = 1$). It is then clear that n', real part of the refractive index, describes *refraction*, namely, the change in speed of light inside the material. In contrast, the imaginary part n'' describes *absorption*, the attenuation of the wave amplitude inside the material.

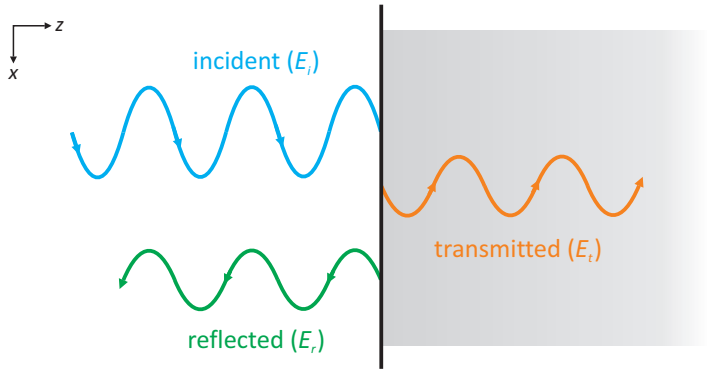

Figure 12.1: Propagation of light at the crystal surface. The incident beam splits into the reflected and transmitted beams. Their intensities are determined by the complex refractive index of the crystal, $n = n' + in''$.

Absorption measurements require a suitably chosen sample thickness, such that the fraction of the absorbed intensity is neither too large nor too small. It is often more convenient to measure *reflectivity*, which is defined as the intensity ratio of the incident and reflected light. In the case of normal incidence, all of the incident, reflected, and transmitted waves travel along the z direction perpendicular to the surface (Fig. 12.1),

$$\begin{aligned} \text{incident:} \quad & E_i = E_{i0}\,e^{i(k_0z-\omega t)} \\ \text{transmitted:} \quad & E_t = E_{t0}\,e^{i(nk_0z-\omega t)} \\ \text{reflected:} \quad & E_r = E_{r0}\,e^{i(-k_0z-\omega t)} \end{aligned}$$

At the interface, which we choose as $z = 0$, electric field should change continuously, so the amplitudes fulfill the condition $E_{t0} = E_{i0} + E_{r0}$. A similar condition should hold for the magnetic field too, $\omega\mathbf{B} = \mathbf{k}\times\mathbf{E}$ according to Eq. (A.8). Therefore,

$$nE_{t0} = E_{i0} - E_{r0}. \tag{12.3}$$

[22] We use primes in these lecture notes, but it is also customary to write $n = n_1 + in_2$ and $\varepsilon = \varepsilon_1 + i\varepsilon_2$.

It is then easy to eliminate E_{t0} and calculate reflectivity,[23]

$$R = \frac{|E_{r0}|^2}{|E_{i0}|^2} = \frac{|1-n|^2}{|1+n|^2}. \tag{12.4}$$

In Ch. 12.4, we will see that R values close to 1 are obtained when n'' is large, whereas n' vanishes. Then any light transmitted through the interface is immediately absorbed, so the sample is non-transparent: no light can go through. In a more general situation, part of the transmitted amplitude, E_{t0}, is then lost due to absorption (A), whereas transmittance of the whole sample is $T = 1 - R - A$.

12.2. Fluctuating dipoles

We now return to the phonons and consider the diatomic chain (Ch. 11.5) where the two atoms not only have different masses but also carry the charges of $+q_e$ and $-q_e$, respectively. At $q = 0$, the optical mode involves opposite displacements of these atoms, such that a fluctuating dipole moment $\mu_d(t)$ is induced by the phonon. Our strategy now will be calculating this dipole moment and the corresponding permittivity ε to obtain the refractive index n and analyze optical response of the crystal. We will do this using a very simple – and, in all honesty, oversimplified – model before drawing an argument why the predictions of this model remain valid in the more general case.

Light features an oscillating electric field, $E \sim e^{-i\omega t}$, that interacts with the charges. Then the force acting on the atoms should be augmented by the Columb force, and the equations of motion from Ch. 11.5 should be revised as

$$\begin{cases} m_1 \frac{d^2 u_p}{dt^2} = -2\mathcal{K}(u_p - v_p) + q_e E_{\text{local}} \\ m_2 \frac{d^2 v_p}{dt^2} = -2\mathcal{K}(v_p - u_p) - q_e E_{\text{local}} \end{cases}$$

The phonon is considered at $q \to 0$, so all atoms of a given type undergo the same displacement, and we end up with only one differential equation for $l = u_p - v_p$, the dipole length. Indeed, dividing the first equation by m_1 and the second equation by m_2 returns the single equation for l,

$$\frac{d^2 l}{dt^2} = -\mathcal{K}\left(\frac{1}{m_1} + \frac{1}{m_2}\right) l + \left(\frac{1}{m_1} + \frac{1}{m_2}\right) q_e E_{\text{local}} \;\Rightarrow\; m \frac{d^2 l}{dt^2} + m\omega_0^2 l = q_e E_{\text{local}}. \tag{12.5}$$

This is a standard equation for a driven harmonic oscillator with $\omega_0 = \sqrt{2\mathcal{K}/m}$, the frequency of the optical phonon at $q = 0$ in the absence of any electric charges (as in Ch. 12).

Electric field is local in the sense of Ch. 10.4. It includes the internal field due to light, as well as Lorenz and depolarization fields, which are proportional to polarization. The polarization oscillates too, following oscillations of the dipole moment $\mu_d = q_e\, l$. Therefore, it makes sense to choose the oscillating form of $E_{\text{local}} = E_0\, e^{-i\omega t}$ and search for the oscillating solution, $l(t) = A\, e^{-i\omega t}$. The result is,

$$A(\omega) = \frac{q_e/m}{\omega_0^2 - \omega^2} E_0 \;\Rightarrow\; \mu_d(t) = q_e\, l(t) = \frac{q_e^2/m}{\omega_0^2 - \omega^2} E_{\text{local}}(t), \tag{12.6}$$

and polarizability of the crystal due to an optical phonon becomes

$$\alpha(\omega) = \frac{q_e^2/m}{\omega_0^2 - \omega^2}. \tag{12.7}$$

[23] This expression is derived for the case of normal incidence. More complex Fresnel equations are required for an arbitrary incidence angle. In particular, polarization of light changes upon the non-90° reflection, which is the cornerstone of the optical method called ellipsometry.

Electric field drives oscillations and creates resonance when its frequency matches the frequency of the system, which is the frequency of the optical phonon at $q \to 0$.

12.3. LO vs. TO

We should now use this polarizability α to calculate optical parameters from Ch. 12.1. Before doing that, let's compare electric polarizations created by the TO and LO phonons. These two types of phonons differ by the direction of their displacements relative to the propagation direction $\mathbf{q}$. The displacements take the form $\mathbf{u} = \mathbf{u}_0\, e^{i(\mathbf{qr}-\omega t)}$ where $\mathbf{q}$ is the chain direction, so we expect $\mathbf{P} = \mathbf{P}_0\, e^{i(\mathbf{qr}-\omega t)}$ with $\mathbf{P} \parallel \mathbf{q}$ (LO) and $\mathbf{P} \perp \mathbf{q}$ (TO).

In the absence of an external electric field, Eq. (10.1) becomes

$$\mathbf{D} = \varepsilon_0 \mathbf{E}_{\text{depol}} + \mathbf{P}, \tag{12.8}$$

and we expect the same wave-like form of $\mathbf{D} = \mathbf{D}_0\, e^{i(\mathbf{qr}-\omega t)}$ and $\mathbf{E}_{\text{delop}} = \mathbf{E}_0\, e^{i(\mathbf{qr}-\omega t)}$ because both of them arise from the same atomic displacements. Additionally, one of Maxwell's equations requires $\text{div}\mathbf{D} = 0 \;\Rightarrow\; \mathbf{D} \cdot \mathbf{q} = 0$. For the LO phonon, this condition holds with $\mathbf{D} = 0$ only, hence $\mathbf{E}_{\text{depol}} = -\mathbf{P}/\varepsilon_0$ corresponding to the depolarization factor $f = 1$. On the other hand, the TO phonon entails $\mathbf{D} \perp \mathbf{q}$ for an arbitrary $\mathbf{D}$ and satisfies the above condition, but another Maxwell's equation, $\text{rot}\,\mathbf{E} = 0$, requires $\mathbf{q} \times \mathbf{E} = 0$, which is possible with $\mathbf{E}_{\text{depol}} = 0$ only because $\mathbf{E}_{\text{depol}} \perp \mathbf{q}$ in this case. Therefore, the TO phonon corresponds to the depolarization factor $f = 0$. Altogether,

$$\text{LO:}\quad E_{\text{local}} = \frac{P}{3\,\varepsilon_0} - \frac{P}{\varepsilon_0} = -\frac{2P}{3\,\varepsilon_0}, \qquad\qquad \text{TO:}\quad E_{\text{local}} = \frac{P}{3\,\varepsilon_0} \tag{12.9}$$

where $P(t)$ is electric polarization created by the fluctuating dipoles $\mu_d(t)$.

Using these expressions in the definition of the electric polarization, $P = n_d \mu_d = n_d \alpha E_{\text{local}}$, one finds simple relations for the LO and TO phonon frequencies

$$P = \frac{n_d q_e^2}{3m\,\varepsilon_0} \frac{-2P}{\omega_0^2 - \omega_{\text{LO}}^2} \quad \Rightarrow \quad \omega_{\text{TO}}^2 = \omega_0^2 - \frac{n_d\, q_e^2}{3m\,\varepsilon_0} \tag{12.10}$$

$$P = \frac{n_d q_e^2}{3m\,\varepsilon_0} \frac{P}{\omega_0^2 - \omega_{\text{TO}}^2} \quad \Rightarrow \quad \omega_{\text{LO}}^2 = \omega_0^2 + \frac{2n_d\, q_e^2}{3m\,\varepsilon_0} \tag{12.11}$$

We thus conclude that $\omega_{\text{LO}} \geq \omega_{\text{TO}}$. The difference between these frequencies gauges ionicity of the crystal. We basically see that atomic charges modify the phonon frequency $\omega_0 = \sqrt{2k/m}$ that has been obtained for neutral atoms. The LO and TO phonons shift charges in different ways and create different local polarizations. The LO phonon separates the charges and creates internal electric fields that counteract the atomic displacements. Therefore, higher energy is required for the LO-type atomic motion.

The oversimplified nature of this model is not to be overlooked, though. We assumed the same stiffness k for the longitudinal and transverse atomic motion, which is of course far from realistic in the light of the differences between the compressional and shear waves (Ch. 11.4). Nevertheless, we will see that even this primitive model does lead to a qualitatively correct physical picture, which justifies the exaggerated approximations involved.

12.4. Interaction with light, polaritons

Expressions (12.10) and (12.11) for the phonon frequencies lead to a convenient simplification of the permittivity, which is obtained via the Clausius-Mosotti relation, Eq. (10.15),

$$\varepsilon(\omega) = \frac{1 + 2n_d\alpha/(3\varepsilon_0)}{1 - n_d\alpha/(3\varepsilon_0)} = \frac{\omega_{\text{LO}}^2 - \omega^2}{\omega_{\text{TO}}^2 - \omega^2} \tag{12.12}$$

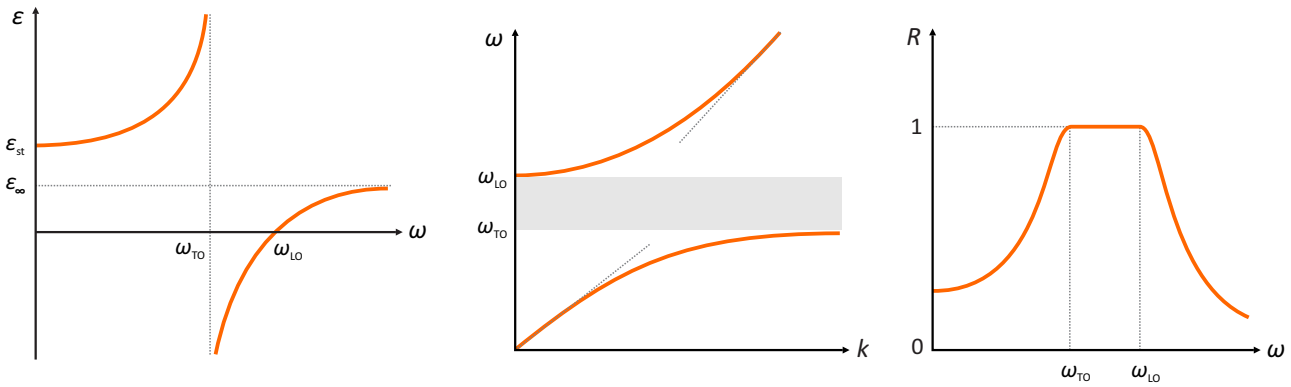

Figure 12.2: Interaction of optical phonon with light. Left: frequency dependence of the permittivity. Middle: polariton dispersion caused by the interaction of light with the phonon. Right: frequency dependence of the reflectivity with the *Reststrahlen* band at $\omega_{\rm TO} < \omega < \omega_{\rm LO}$.

The conjectured frequency ω_0 disappears, and only the tangible frequencies, $\omega_{\rm TO}$ and $\omega_{\rm LO}$, remain. Permittivity diverges at $\omega = \omega_{\rm TO}$ and shows a zero crossing at $\omega = \omega_{\rm LO}$ (Fig. 12.2, left).

This form of the permittivity modifies an electromagnetic wave at frequencies near $\omega_{\rm TO}$ and $\omega_{\rm LO}$. Indeed, by using Eq. (12.12) in the dispersion relation, Eq. (12.1), one finds that the standard linear dispersion $\omega \sim k$ does not hold in the vicinity of the phonon frequency, and no real solution exists for $\omega(k)$ at $\omega_{\rm TO} \le \omega < \omega_{\rm LO}$. It means that photons can not propagate in the crystal within this frequency range. The characteristic dispersion shown in Fig. 12.2 (middle) is often ascribed to a *polariton*, an electromagnetic wave strongly coupled to an intrinsic and dipole-carrying excitation of the crystal.

The polariton formation causes the crystal to reflect electromagnetic waves. Indeed, at $\omega < \omega_{\rm TO}$ and at $\omega > \omega_{\rm LO}$, one finds $\varepsilon > 0$, such that $n = n' + in''$ is a real number with $n' \neq 0$ and $n'' = 0$. Crystal refracts light, as we know from NaCl, quartz, and many other ionic crystals. On the other hand, at $\omega_{\rm TO} < \omega < \omega_{\rm LO}$, negative ε renders n a purely imaginary number with $n' = 0$ and $n'' \neq 0$.[24] The resulting reflectivity is

$$R = \frac{|1 - in''|^2}{|1 + in''|^2} = 1, \tag{12.13}$$

so ionic crystals reflect light in the frequency range between $\omega_{\rm TO}$ and $\omega_{\rm LO}$ (Fig. 12.2, right). These so-called *Reststrahlen bands* are observed, for example, in ionic crystals in the infrared range ($\omega = 0.3 - 400\,$THz) typical for optical phonons. A similar mechanism underlies the response of polar molecules that absorb infrared radiation at frequencies of their vibrational modes.

12.5. Lyddane-Sachs-Teller relation

Eq. (12.12) returns the low-frequency (static) limit of $\varepsilon_{\rm st} = \omega_{\rm LO}^2/\omega_{\rm TO}^2$ and the high-frequency limit of 1. Practically, however, more than one optical phonon is usually present in the crystal, so this high-frequency limit of one phonon mode will be the low-frequency limit of another one with a higher energy. Moreover, beyond all phonon frequencies one still expects electronic excitations at energies of $E = 10^0 - 10^4\,$eV. Therefore, it is customary to introduce $\varepsilon_\infty \neq 1$ and

[24] This distinction between the purely real and purely imaginary n is, of course, a drawback of our naive approximation. The purely real $\varepsilon(\omega)$ arises from the purely real $\alpha(\omega)$ obtained in Ch. 12.2 from the equations of motion that did not include any damping term. Realistically, damping creates a phase shift between $\mu_d(t)$ and $E_{\rm local}(t)$, thus rendering all optical parameters complex numbers.

write permittivity as[25]

$$\varepsilon(\omega) = \varepsilon_\infty \frac{\omega_{\rm LO}^2 - \omega^2}{\omega_{\rm TO}^2 - \omega^2}, \tag{12.14}$$

resulting in

$$\frac{\varepsilon_{\rm st}}{\varepsilon_\infty} = \frac{\omega_{\rm LO}^2}{\omega_{\rm TO}^2}, \tag{12.15}$$

the *Lyddane-Sachs-Teller relation*.

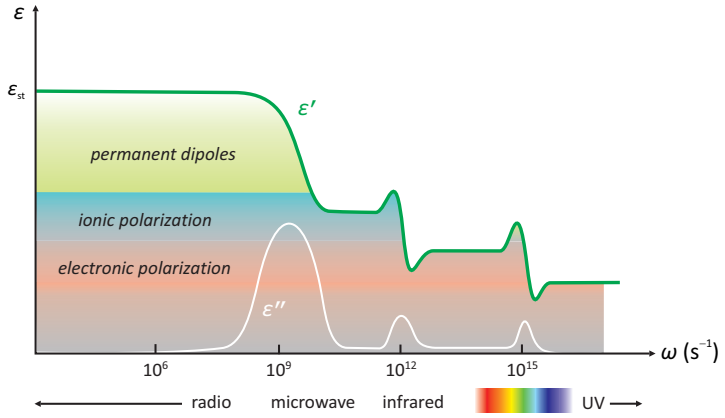

Figure 12.3: Schematic representation of different contributions to the permittivity. Re-orientation of permanent dipoles at low frequencies (Fig. 10.2, right) is followed by the ionic polarization due to phonons and eventually by the electronic polarization due to induced dipoles within individual atoms. Electronic and ionic relaxations give rise to wiggles, which are broadened versions of the divergence of $\varepsilon(\omega)$ shown in Fig. 12.2 (left).

An interesting outcome of this analysis is that static permittivity of a crystal is determined by its phonon frequencies. Even a nonpolar crystal without any permanent dipoles may show $\varepsilon_{\rm st}$ well above 1.0 because charges inside the crystal move as a result of the atomic motion. A crystal with permanent dipoles shows an additional contribution to $\varepsilon_{\rm st}$ due to these pre-existing dipoles. Then, $\varepsilon_{\rm st}$ of the Lyddane-Sachs-Teller relation is ε_∞ of the Debye relaxation (Ch. 10.6). Different contributions to the permittivity are sketched in Fig. 12.3.

12.6. Infra-red active phonon modes

While the appealing form of the permittivity, Eq. (12.12), is the result of several simplifications introduced in our model (linear chain, same spring constant for the longitudinal and transverse displacements), the qualitative behavior displayed in Fig. 12.2 is quite general. We can see this by re-iterating the arguments from Ch. 12.3 but now considering a displacement wave in the crystal triggered by the oscillating electric field of light. Assume that the electric field $\mathbf{E} = \mathbf{E}_0\, e^{i(\mathbf{kr}-\omega t)}$ generates the polarization $\mathbf{P} = \mathbf{P}_0\, e^{i(\mathbf{kr}-\omega t)}$ and the displacement field $\mathbf{D} = \mathbf{D}_0\, e^{i(\mathbf{kr}-\omega t)}$. According to Maxwell's equations,

$$\operatorname{div}\mathbf{D} = 0 \quad \text{and} \quad \operatorname{rot}\mathbf{E} = 0 \quad \Rightarrow \quad \mathbf{k}\cdot\mathbf{D} = 0 \quad \text{and} \quad \mathbf{k}\times\mathbf{E} = 0. \tag{12.16}$$

The former condition requires $\mathbf{D} = 0$ or $\mathbf{k} \perp \mathbf{D}$ (hence $\mathbf{k} \perp \mathbf{E}$), while the latter requires $\mathbf{E} = 0$ or $\mathbf{k} \parallel \mathbf{E}$ (hence $\mathbf{k} \parallel \mathbf{D}$).

Consider the TO phonon. In this case, $\mathbf{D} \perp \mathbf{k}$, so $\mathbf{E}$ must be zero for the second condition to be fulfilled. Then, $\varepsilon \to \infty$ because $\mathbf{D} = \varepsilon\varepsilon_0\mathbf{E}$, so $\varepsilon(\omega)$ diverges at $\omega_{\rm TO}$. On the other hand, the LO phonon implies $\mathbf{E}\|\mathbf{k}$, so $\mathbf{D}$ must be zero, which is only possible at $\varepsilon = 0$. Therefore, a zero crossing of $\varepsilon(\omega)$ should occur at $\omega_{\rm LO}$. The pre-condition for these arguments is our assumption that $\mathbf{D} \parallel \mathbf{E}$ or, basically, the diagonal form of the permittivity tensor expected in crystals with the sufficiently high symmetry (Ch. 2.5).

[25] This equation can be obtained rigorously by augmenting the ionic polarizability in Eq. (12.7) with the atomic polarizability α_0 as the origin of $\varepsilon_\infty \neq 1$. Unfortunately, this small amendment leads to a far more tedious algebra than what we did here, so this exercise is recommended for nerds only.

The situation becomes more complex in crystals with lower symmetry. Indeed, even distinguishing between longitudinal and transverse phonons is not possible in this case, because atomic displacements are not constrained to be parallel or perpendicular to the propagation vector of the phonon (see also Ch. 13). However, what matters for our analysis is not $\mathbf{q}$ but $\mathbf{k}$, the propagation direction of light. One can think of splitting atomic displacements of an arbitrary phonon mode into two components. The component perpendicular to $\mathbf{k}$ leads to a divergence of $\varepsilon(\omega)$ at $\omega = \omega_{\mathrm{TO}}$, whereas the component parallel to $\mathbf{k}$ results in the zero crossing at some effective frequency $\omega = \omega_{\mathrm{LO}}$.

It may seem that almost every phonon mode of a non-cubic crystal should show up in $\varepsilon(\omega)$ and in the optical (infrared) spectrum. Not quite. No coupling to light occurs when phonon mode does not generate any dipole moment. This may happen in a covalent crystal or when the phonon preserves inversion symmetry.[26] What ultimately matters is the formation of a dipole moment (i.e., atomic displacements) parallel to $\mathbf{E}$ of light. The coupling between this dipole moment and oscillating electric field renders phonon-mode *IR-active*. Polarized light is often used to single out modes with a given direction of the atomic displacements.

[26] Such modes are called *even* (*gerade*), in contrast to *odd* (*ungerade*) modes that break the inversion symmetry. For a given crystal, the distribution of modes into odd and even can be analyzed on the basis of crystal symmetry and occupied Wyckoff positions, for example using the SAM utility at the Bilbao server.

13. Phonons and the reciprocal lattice

13.1. Brillouin zone

13.2. Dynamical matrix

...

A. Electrodynamics

A.1. Maxwell's equations

For a non-magnetic solid one writes the four *Maxwell's equations* in the form

$$\operatorname{div} \mathbf{D} = \rho_e, \tag{A.1}$$

$$\operatorname{div} \mathbf{B} = 0, \tag{A.2}$$

$$\operatorname{rot} \mathbf{E} + \frac{\partial \mathbf{B}}{\partial t} = 0, \tag{A.3}$$

$$\operatorname{rot} \mathbf{H} - \frac{\partial \mathbf{D}}{\partial t} = \boldsymbol{j}, \tag{A.4}$$

where ρ_e is the charge density and $\boldsymbol{j}$ is electric current density. The displacement field $\mathbf{D} = \varepsilon\varepsilon_0\mathbf{E}$ is defined via the permittivity ε, while the two magnetic fields are related by $\mathbf{B} = \mu_0\mathbf{H}$.

One can also derive the *continuity equation* by taking divergence of Eq. (A.4) and using the vector identity $\operatorname{div}(\operatorname{rot}\mathbf{H}) = 0$,

$$\operatorname{div}(\operatorname{rot}\mathbf{H}) - \frac{\partial}{\partial t}\operatorname{div}\mathbf{D} = \operatorname{div}\boldsymbol{j} \quad \Rightarrow \quad \operatorname{div}\boldsymbol{j} + \frac{\partial \rho_e}{\partial t} = 0. \tag{A.5}$$

It shows that any change in the charge density is caused by the flux of the electric current, and vice versa.

The above equations are written in the SI units where $\varepsilon_0 = 8.85 \times 10^{12}\,\mathrm{C/(V\,m)}$ and $\mu_0 = 4\pi \times 10^{-7}\,\mathrm{V\,s/(A\,m)}$ are the vacuum permittivity and permeability, respectively. It is not advisable to use CGS units unless you really have to, because Maxwell's equations will contain additional pre-factors in this case.

A.2. Electromagnetic waves

A solution to Maxwell's equations can be found in the form of plane waves,

$$\mathbf{E} = \mathbf{E}_0\, e^{i(\mathbf{kr}-\omega t)}, \qquad \mathbf{B} = \mathbf{B}_0\, e^{i(\mathbf{kr}-\omega t)}, \tag{A.6}$$

where $\mathbf{k}$ is the propagation vector and amplitudes $\mathbf{E}_0$, $\mathbf{H}_0$ can be complex to allow for a phase shift between $\mathbf{E}$ and $\mathbf{B}$. By replacing Eqs. (A.6) into the Maxwell's equations, one finds

$$\varepsilon\varepsilon_0\,(\mathbf{k}\cdot\mathbf{E}) = 0 \qquad \mu_0\,(\mathbf{k}\cdot\mathbf{H}) = 0 \tag{A.7}$$

$$\mathbf{k}\times\mathbf{E} = \omega\mathbf{B} \qquad \mathbf{k}\times\mathbf{H} + \varepsilon\varepsilon_0\omega\,\mathbf{E} = \boldsymbol{j}/i. \tag{A.8}$$

The current $\boldsymbol{j}$ can be eliminated using Ohm's law, $\boldsymbol{j} = \sigma\mathbf{E}$, which transforms Eq. (A.8) into

$$\mathbf{k}\times\mathbf{H} = -(\varepsilon\varepsilon_0\omega + i\sigma)\,\mathbf{E}. \tag{A.9}$$

The most natural solution to Eqs. (A.7)–(A.8) is the transverse wave with $\mathbf{k}\perp\mathbf{E}$ and $\mathbf{k}\perp\mathbf{B}$, thus satisfying Eqs. (A.7). From the remaining two equations one concludes that $\mathbf{E}\perp\mathbf{B}$. This way, $\mathbf{E}$ and $\mathbf{B}$ oscillate along two different (orthogonal) directions, whereas the wave propagates along the third one. It is the standard *electromagnetic wave* (light) as we know it.

To explore the behavior of such transverse waves, we use the vector relation

$$\mathbf{k}\times[\mathbf{k}\times\mathbf{E}] = \mathbf{k}(\mathbf{k}\cdot\mathbf{E}) - (\mathbf{k}\cdot\mathbf{k})\mathbf{E} = -\mathbf{k}^2\mathbf{E}$$

($\mathbf{k}\cdot\mathbf{E}=0$ since the two vectors are orthogonal) and apply it to Eqs. (A.8). Then we obtain

$$-\mathbf{k}^2\,\mathbf{E} = -\mu_0\omega(\varepsilon\varepsilon_0\omega + i\sigma)\,\mathbf{E}$$

and arrive at the *dispersion relation*

$$k^2 - \varepsilon\varepsilon_0\mu_0\,\omega^2 - i\mu_0\sigma\,\omega = 0 \tag{A.10}$$

that is usually written in a more concise linear form,

$$c^2k^2 = \hat{\varepsilon}(\omega)\,\omega^2, \tag{A.11}$$

with $c = 1/\sqrt{\varepsilon_0\mu_0} = 3\times10^8\,\mathrm{m/s}$, speed of light in vacuum, and complex permittivity

$$\varepsilon(\omega) = \varepsilon + \frac{i\sigma}{\varepsilon_0\omega}. \tag{A.12}$$

It is what we call permittivity throughout these lecture notes. The practical advantage of the complex permittivity is the simple and convenient linear dispersion relation, $k\sim\omega$. The conceptual physical reason for merging permittivity and conductivity into a single parameter is that both of them describe system's response to the electric field, but charge displacements (ε) have a phase shift of $\pi/2$ with respect to charge velocities (σ). Ch. **??** offers some further insights into this issue.

A.3. Longitudinal waves

Another solution of Eqs. (A.7)–(A.8) exists when $\varepsilon = 0$. Then the first equation of Eq. (A.7) is fulfilled for any $\mathbf{k}$ and $\mathbf{E}$. Specifically, a non-magnetic solution ($\mathbf{B}=0$) becomes possible when $\mathbf{k}\parallel\mathbf{E}$, with no other restrictions imposed on k, whereas frequency is determined by the $\varepsilon = 0$ condition. This solution is a longitudinal wave, where electric field oscillates along the propagation direction. It does not occur in vacuum where $\varepsilon = 1$, but it may occur in medium when ε is tuned to zero. This is one way to see the LO phonon (Ch. 12.3) as well as plasmons in metals (Ch. **??**).

B. Thermodynamics

C. List of experimental techniques